ISAS - INTERNATIONAL SCHOOL
FOR ADVANCED STUDIES

Electrophysiology of Xenopus oocytes as a Method for the Study of Membrane Proteins Structure and Functions

Thesis Submitted for the Degree of
Magister Philosophiae

Candidate: Lia Chiara Forti

Supervisors: Dr. Oscar Moran
Prof. Antonio Borsellino

Academic Year 1989/90

TRIESTE

SISSA - SCUOLA
INTERNAZIONALE
SUPERIORE
DI STUDI AVANZATI
TRIESTE
Strada Costiera 11

Index

Chapter 1

Introduction

Biological membranes are mainly formed by lipids and proteins. In the study of the molecular structure of membranes thus a great importance has the study of membrane proteins structure. This field presents many more problems than the study of proteins in acqueous solution: in fact, the functional performances, and with most probability the favoured conformations, of a membrane protein, are conditioned by its insertion in a membrane. This property opposes a large number of technical problems to the experimental access to membrane proteins.

Depending on particular cases, different methods have been applied to the study of membrane proteins structure and function: biochemical and immunological methods, cristallography, various spectroscopic methods, electrophysiology.

A new prospective in the field is offered by the interaction of molecular genetics, biochemistry and electrophysiology. In the light of this interaction special techniques have been developed that enable the utilization in membrane protein research of the clones of genes coding for such proteins, clones being obtained through molecular genetics techniques.

The work carried out in this thesis consists in the design and construction of the experimental set–up needed to implement one of the above cited techniques, namely the expression in oocytes, a technique that essentially involves genetics and electrophysiology. We have been mainly involved in the electrophysiological part of the oocyte expression technique.

The electrophysiological characterization of membrane proteins is supported by a well established theoretical and experimental background on the electrical activity of biological membranes. An overview of this background will be exposed in the rest of this introduction. An introduction to the technique of expression in oocytes and to its role in the investigation of membrane proteins structure and functions is presented in chapter 2. Chapters 3 and 4 expose the fundamentals of the voltage clamp technique, which is one of the main tools in electrophysiology; the steps in the construction of a voltage clamp amplifier for *Xenopus* oocytes will be also illustrated, as this construction took a considerable part in our work. Chapters 5 and 6 describe various steps in the experimental method and some test measurements.

1.1 Electrical properties of biological membranes

There is a charge separation and an electrical field across any biological membrane delimiting a living cell.

This is seen by measuring with an electrode the electrical potential difference between the internal and the external side of the membrane: it is usually around -60 to -80 mV, internal potential minus external potential. For the so called excitable cells, such as neurons and muscles, the potential difference can be seen to change transiently after electrical or appropriated chemical stimulation.

This electrical activity, observed long time ago, has suggested a model of cell membranes as elements of an electrical circuit, characterized by a specific resistance and capacity. Moreover the existence of a resting non zero membrane potential has suggested the presence in the membrane of the equivalent of a battery, whose physical consistency is nowadays identified with the so called active transport systems.

The active transport systems are membrane constituents able to keep a constant non zero concentration gradient across the membrane for a few different species of permeant ions, thus producing a non–equilibrium steady electrochemical potential gradient.

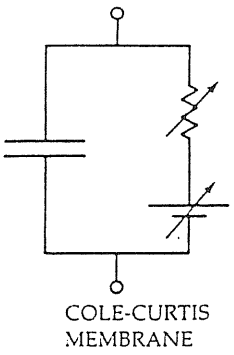

Fig. 1.1: Equivalent circuit used by Cole and Curtis (1938) to interpret their measurements of membrane impedance during the propagated action potential.

A scheme like the one in fig. 1.1 was proposed early in this century (Cole and Curtis, 1938) as an equivalent electrical model for the local behaviour of a piece of membrane. Many evidences had proven that the membranes have a fairly constant capacity of about 1 $\mu F/\ cm^2$ (Cole, 1972).

As far as a resistance is concerned, a variable resistance in the nerve and muscle membrane had been first hypothesized in the famous Bernstein hypothesys (1902), and then measured, before the development of the voltage clamp (see chapter 3), by Cole and Curtis (1938), who saw a big increase (40 times) in membrane conductance during the nerve action potential.

It is worth to remind that the term resistance derives in origin from the theory of linear electrical circuits. A linear circuit with concentrated components is such that a set of linear ordinary differential equations can be assumed to describe the time evolution of the current and voltage at any node in the circuit.

The main practical implication of linearity is that, if at least one resistance is present in the circuit, the current at any node in response to a steady potential, applied at any other node at time 0, relaxes to a steady value, and the steady state current vs. voltage (I–V) relation is linear (Ohm's law).

The slope of the I–V straight line, called the conductance (inverse resistance), is a constant parameter describing the circuit between the points

where V is applied and I is measured. In the electrophysiological terminology, a membrane behaving as a linear circuit is commonly called 'passive'.

By contrary, in a non linear electrical circuit the above definition of resistance can not be applied, as the I–V relations are generally not any more straight lines, at any time.

The names 'resistance' and 'conductance' are still used, but they have to be redefined. If a current is a generic function of potential V and time t, $I = I(V,t)$, then the chord conductance $G_c(V,t)$ at time t is defined as

$$G_c(V,t) \equiv \frac{I(V,t)}{V - V_{rest}}$$

where V_{rest} is the steady state zero–current potential, $I(V_{rest}, t = \infty) = 0$. In the case of a membrane, by the way, there is usually one zero–current stable potential.

Alternatively, one can define the slope conductance at time t, $G_s(V,t)$, as

$$G_s(V,t) \equiv \frac{\partial I(V,t)}{\partial V} \quad .$$

The chord and slope conductances are thus variable with V and t.

In a cell plasma membrane it is evident, by inspection of the I–V curves obtained by voltage clamping (see chapter 3), that: a) the membrane current response to an applied membrane potential V is generally non–linear with V at any time, or equivalently the membrane slope conductance varies with V; and b) the time dependence of I after applying a V value is variable from membrane to membrane and is also variable for one membrane in dependence of its past history.

The explanation of these nonlinearities is a main subject of membrane electrophysiology, because it requires a description of the membrane structure and of the physical basis of electrical conduction across membranes.

The electrophysiological studies have proposed, and partially answered to, the following questions:

i) which kind of non linear electrical model circuit can we adopt for reproducing the experimental I–V characteristics of a membrane?

ii) what are the charge carriers in the membrane current?

iii) which are the physical structures in the membrane correlated with the model electrical components such as variable resistances and capacitors?

An answer to question *i)* was given, in the case of the squid axon membrane, by the classical work of Hodgkin and Huxley (1952), in which they proposed, as a model for local current fluxes across a piece of membrane, the electrical circuit in fig. 1.2, with g_{Na} and g_K varying with membrane potential V and time t. They formulated, on the basis of their experimental observations, the analytical laws relating the model parameters g_{Na} and g_K to V and t.

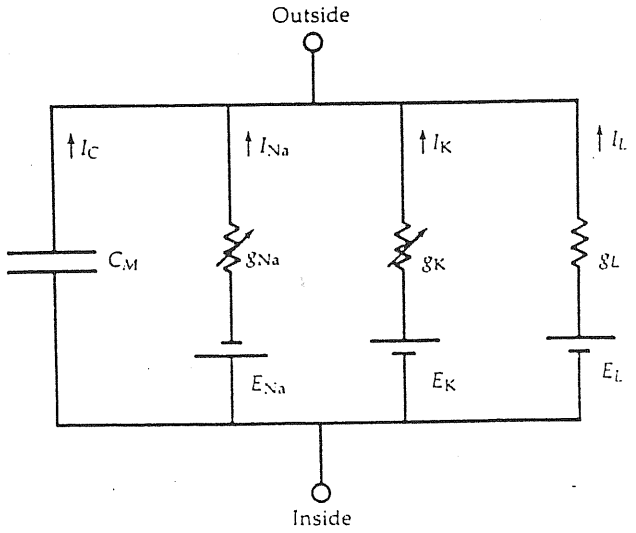

Fig. 1.2. The equivalent electrical circuit for the axon membrane proposed by Hodgkin and Huxley (1952).

The proposal was consistent, as in fact with appropriated initial conditions the squid axon action potential was correctly simulated in their model circuit by the numerical solution for V.

g_{Na} and g_K represent the conductances of branches with selective conduction for the ions sodium and potassium. g_l is the conductance of a

branch with non–selective ionic conduction called 'leak': it is experimentally found to be a constant, independent of voltage and time.

The e.m.f.'s E_{Na}, E_K, E_l are the Nernst potentials for sodium and potassium for assigned concentration gradients across the membrane, and the zero–current potential for the leak conductance.

A generalization of the Hodgkin–Huxley picture of the membrane circuit is still used to analyze the macroscopic I–V relations that one obtains applying, for example, the voltage clamp technique.

For what concerns points *ii)* and *iii)*, it is believed nowadays that the electric currents across the membranes are carried by ions, mainly Na^+, K^+ and Cl^-. The membrane permeability, defined empirically as minus the ratio of ionic flux over concentration gradient, differs from ion to ion.

The ionic fluxes through an homogeneous selectively permeable membrane near steady state can be described by the classical Nernst–Planck electrodiffusion equation. The most common approximation for thin membranes are the Goldman–Hodgkin–Katz (GHK) 'constant field' equations (see for example Finkelstein and Mauro, 1977). The GHK equation for the current carried by ion i is:

$$I_i = zFP_iU\frac{c_i \exp U - c_o}{\exp U - 1} \tag{1.1}$$

where P_i is the permeability of ion i, z is its valence, F is the Faraday constant, $U \equiv zFV/RT$, with R the gas constant and T the absolute temperature; c_i and c_o are the internal and external concentration respectively of ion i. The total current across the membrane is $I_{tot} = \sum_i I_i$, and the zero current potential V_{rest} (or resting potential) is determined by (if the permeant ions are Na^+, K^+ and Cl^-):

$$V_{rest} = \frac{RT}{F}\ln\frac{P_{Na}[Na^+]_o + P_K[K^+]_o + P_{Cl}[Cl^-]_i}{P_{Na}[Na^+]_i + P_K[K^+]_i + P_{Cl}[Cl^-]_o} \tag{1.2}$$

where the subscripts $_i$ and $_o$ indicate the intracellular and extracellular concentrations respectively. This equation is useful in studying the membrane ionic permeabilities when the ionic concentrations are known (for an example see seection 6.1); however the GHK equations are derived for homogeneous selective membranes.

It is believed instead that for biological membranes the ionic permeabilities do not represent a property of an homogeneous membrane. The ionic currents flow mainly through low–density, sparse pores in the membrane filled with acqueous solution. The pores are produced by specialized 'channel' proteins. These proteins often very selectively allow only one kind of ion to pass through, and they present a variable resistance to the ionic electrodiffusive flux, in dependence of the conformational state of the protein itself. The actual conformational state can vary as a consequence of electrical or chemical variations of the channel environment.

The many findings supporting this description of membrane electrical activity are examined exaustively by Hille (1984).

Chapter 2

The expression in oocytes of foreign membrane proteins as a tool to membrane biology

2.1 Expression systems: the Xenopus oocyte

The many different applications of the molecular biology techniques have required the development of expression systems for endogenous or cDNA transcribed mRNA. In an expression system a given mRNA sequence is translated into the corresponding aminoacidic sequence due to the work of the translational biosynthetic apparatus of the expression system itself.

Depending on the expression system, some of the steps of the post–translational processing of the expressed protein are carried on, and eventually a functional protein is obtained.

The expression systems that are nowadays used go from the cell–free systems like the rabbit reticulocyte lisate or the wheat germ system, to cellular systems, among which *Escherichia Coli, Xenopus* oocytes, yeast, and cultured cell lines as the mouse fibroblast L cells (see Claudio, 1989).

In the case of membrane proteins, the cell–free translation systems have only a limited utility, because no functional channels, receptors, active transport systems etc. can obviously be obtained in the absence of a membrane. However the cell–free systems have the advantage of synthetizing the required protein in a very short time. Thus their use has been that of a

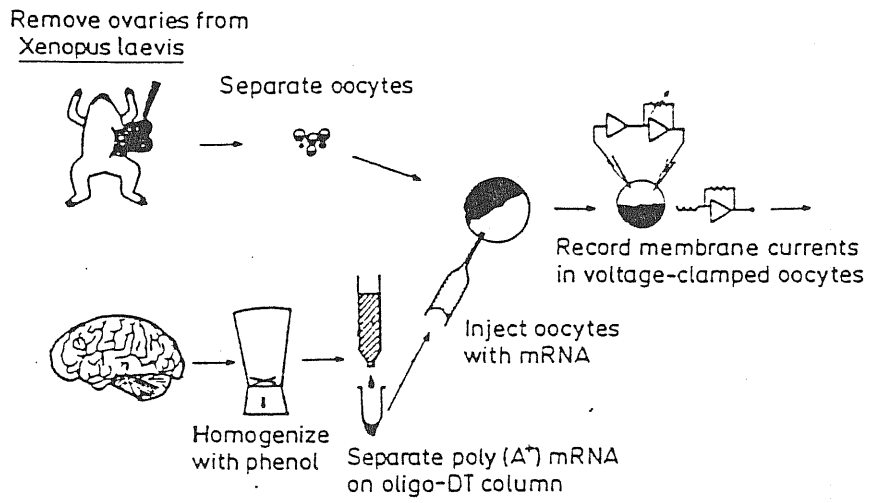

Fig. 2.1: Stages of the transplantation of neurotransmitter receptors into oocytes by the isolation and injection of mRNA from brain (from Sumikawa et al., 1986).

preliminary tool in the search for novel clones, to determine if a candidate RNA sequence has produced for example an appropriately sized polypeptide.

The *Xenopus* oocyte has been used first as expression system for the study of rabbit globins in 1971 (Gurdon et al., 1971). Later it was demonstrated that the oocytes injected with poly$(A)^+$ mRNA extracted from *Torpedo* electric organ efficiently assembled a multi–subunit nicotinic acetylcholine receptor (nAChR) with properties characteristics of the native nAChR (Sumikawa et al., 1981).

Subsequently, the *Xenopus* oocyte has become a standard expression system for the electrophysiological study of neurotransmitter receptors and ionic channels (for reviews see Miledi et al., 1989; Barnard and Bilbe, 1987).

The *Xenopus* oocytes can be injected with either poly$(A)^+$ mRNA extracted from an homogenized tissue on oligo–dT affinity chromatography columns (fig. 2.1) or with the mRNA transcription of a cloned gene. Both kind of experiment are useful at different stages of the investigation on a protein structure. Then after a variable incubation period (from 3 hours to 5 days) the expression of the gene of interest can be assessed, either with biochemical or electrophysiological methods.

The electrophysiological methods used up to now for recording from injected oocytes include voltage clamp (standard two–microelectrode voltage clamp, see section 3.3 in this thesis) and patch clamp, including the possibility of single channel recordings (Miledi et al., 1983; Methfessel et al., 1986).

Detailed accounts of the technical procedures for poly$(A)^+$ mRNA extraction, eventual partial purification, and injection in oocytes can be found in Barnard and Bilbe (1987) and Sumikawa et al. (1989). Accounts on the various voltage clamping and patch clamping procedures are found in the papers by Sumikawa et al. (1989) and Methfessel et al. (1986).

The main advantage of the oocyte expression system comes from the fact that the oocyte has been demonstrated capable of many post–translational modifications for various foreign proteins, as for example signal peptide removal, polyprotein cleavage, N–glycosylation, proline hydroxilation, amino–acetylation and phosphorilation. For what concerns membrane proteins, the oocyte can execute all the assembly processes including the functional insertion of the final product in the membrane, as was first observed for the case of nAChR (Sumikawa et al., 1981) and later confirmed for any vertebrate receptor and channel.

Moreover, as a resting germ cell, the immature oocyte contains very few native receptors and ionic channels. Thus after expression of foreign mRNAs the recorded currents can quite safely be attributed to transplanted channels or receptors, as generally the current amplitudes show a huge increase if compared to the native ones.

2.2 Aims of membrane channels and receptors expression in oocytes

There are several aims for which the expression in oocyte of functional membrane proteins can be a valuable tool. We shall summarize some of them and report some classical examples.

i) The *Xenopus* oocyte offer the possibility to isolate a functional receptor or channel of interest in a controlled and easily accessible environment.

The expressed protein are embedded in a membrane and disposable for electrophysiological recordings, while the difficulties sometimes encountered in the native environment are overcome (e.g. physical difficulty of gaining access to very small neurons or dendrites, imperfect voltage clamping of convoluted structures, damages due to pipette insertion in very small neurons, multiple interacting receptor and channel systems, spontaneous release systems present in neuronal cultures).

ii) The expression in oocyte of poly$(A)^+$ mRNA can help in cloning a membrane protein without previously purifying the protein and determining a part of its primary sequence. One can for example extract poly$(A)^+$ mRNA from a tissue known to be producing in great amount a given receptor of interest. The poly$(A)^+$ mRNA can be fractionated by sucrose sedimentation, and by injecting separately in the oocytes the different fractions one can assess which fraction or fractions are needed to reconstitute the functional receptor (see for example Sumikawa et al., 1984). The selected fractions, enriched in the sequence coding for the receptor, even if containing also other messages, can be utilized to prepare a cDNA library. This latter can in turn be screened by segregating groups of sequences, then again injecting in the oocytes the mRNAs transcribed from the different groups of sequences and waiting for expression. The presence in an oocyte of the fully functional receptor is then the signal that the corresponding group of cDNAs contains the gene of interest. By iterating the procedure after subdivision of the positive group of cDNA sequences, one can arrive in principle to the isolation of the receptor's clone. Examples of the successfull application of this method are the isolation of the serotonin receptor (Lubbert et al., 1987) and the substance K receptor (Maru et al., 1987).

iii) The expression in oocyte offers a fundamental approach to

a) testing the biological functionality of a cloned gene supposed to code for a membrane channel, receptor or other protein. The cloning of a K^+ A–type channel as the product of the *Shaker* gene in *Drosophila* muscle has for example been assessed by expression in *Xenopus* (Timpe et al., 1988).

b) testing if in a cloned receptor all the subunits cloned are necessary and

sufficient for the functional expression of the receptor. In the case of voltage gated channels up to now the cloned structures consisted of only one subunit, and it is not known if they are assembled as omo–oligomers or just as monomers.

A classic example comes from the work of Mishina et al. (1984). From previous works this group disposed of the separate clones for the α, β, γ and δ subunits of the nAChR, which is known to be a pentamer $\alpha_2\beta\gamma\delta$ including the acetylcholine binding site and the associated channel. With expression experiments in oocyte in which different combinations of the α, β, γ and δ subunits mRNAs were used for injection, it was concluded that the presence of the four subunits is required for a fully functional receptor (for a review on nAChR studies, see Claudio, 1989).

c) inquiring in the correlation of a protein structure to its function. A very good method for such inquiries is to obtain the clone and the sequence of the wild type gene coding for e.g. a receptor, and also of the gene corresponding to an altered phenotype. Than the two sequences can be compared, and one can attempt to understand how, in the wild type and mutated protein, structural differencies are related to functional ones. If natural mutants are not available, one can produce artificially specific or random mutations in a cloned sequence, and then determine, through expression in oocytes, how the structure or function of the protein has been altered.

One of the first important applications of this site–directed mutagenesis has been involved with the determination of the role of particular sequences of aminoacids in AchR–channel function, and in particular to search for the channel–lining region (Mishina et al., 1985). For examples of the results obtained with this methods in the study of the structure and functions of voltage operated channels and other channels and receptors in *Drosophila* and other organisms, see Ganetzky and Wu (1989).

iv) A measurement of the relative abundance of specific mRNAs in different tissues and at different stages of development can be performed using expression in oocytes.

The poly$(A)^+$ mRNA can be extracted from the different tissues and injected in oocytes, without any previous purification. Thus the relative amplitude of the currents produced by a given neurotransmitter application, for example, is a measurement of the number of specific functional receptors expressed in the membrane. This is related with the amount of specific mRNA injected, and consequently with the specific mRNA content of the original tissue. In this way maps of a receptor's density distribution can be formed.

v) It is possible to study in the oocyte system the post–translational assembly processes that bring to the formation of functional receptors and channels. This can be done for example by observing the effect on the final expression product of substances known to affect different steps of the assembly process.

An example is given by the study of the effects of tunicamycin inhibition of the N–glycosylation process during the expression of various neurotransmitter receptors and voltage operated channels (Sumikawa et al., 1988; Sumikawa and Miledi, 1989). N–glycosylation is the process of addition of an oligosaccharide group to an asparagine residue in a protein through a glycosidic bond. The addition of sugars to a membrane protein often contributes to ensure correct charge, conformation and stability to a maturing protein, and correct membrane insertion. Tunicamycin blocks N–glycosylation, so that it was possible to assess which membrane proteins needed the glycosylation process for their functional expression.

One could also study the effect of removing, adding or transposing putative regulatory DNA sequences related to a given gene, so as to clarify the regulation of expression and the tissue specificity of expression of the membrane constituents.

vi) Finally, the developing and testing of drugs active on the membrane receptors can also be performed with oocyte expression experiments, even if for such pharmacological studies the expression in permanently transfected cell lines is even better suited.

Chapter 3

Voltage clamping

3.1 The voltage clamp technique

The voltage clamp technique was invented in 1949 by K.Cole (Cole, 1949) and by Marmont (Marmont, 1949). It was successfully applied to the study of the squid axon membrane by Hodgkin, Huxley and Katz in 1952 (Hodgkin et al., 1952). Subsequently, voltage clamping has been applied to many different biological membranes from different tissues, in different animals and in plants. To apply the basic principle of voltage clamping to different membranes, many variations and refinements of the original technique were invented.

The technique plays an important role in the development of electrophysiology, because it has opened the possibility to achieve a major goal, consisting in the separation of the total membrane current associated to a given change in membrane potential into two contributions: the capacitative current due to the charging process of the membrane capacitance, and a second contribution, a resistive current, due to the membrane permeability to some ions.

It is very simple to see how this possibility arises: to "voltage clamp" means to force the membrane potential to be equal to a command value by means of an electronic feedback system. If the command voltage is a sequence of pulses (see fig 3.1)

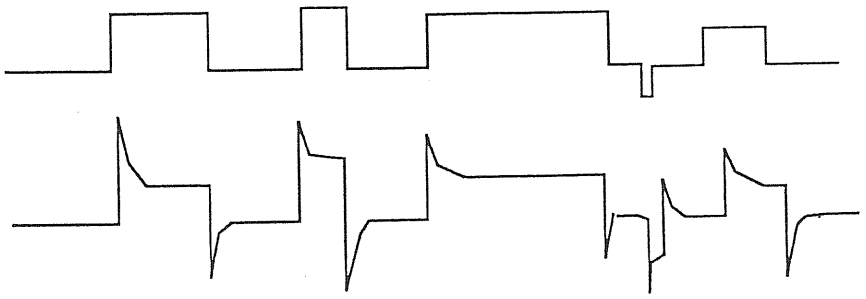

Fig. 3.1. A simulation of a sequence of voltage pulses applied to a membrane (upper trace) and the corresponding membrane current response (lower trace) showing the characteristic capacitative peaks following every potential step variation. See also section 6.1.3

then the membrane potential is maintained constant during the pulses, varying just in the finite time interval needed to move it to the new command value at the onset and end of each pulse. If the equivalent circuit for a piece of membrane (see section 1.1) is assumed to be the one in fig. 1.1, then the total current through that piece of membrane is

$$I_{tot}(t) = C_m \frac{dV(t)}{dt} + I_r(t)$$

where C_m is the membrane capacity, $I_r(t)$ is the current through the resistive branches and $V(t)$ is the membrane potential. When the potential $V(t)$ is constant, the capacitative contribution is null.

In the rest of this chapter, a general decription of the operation principles of a feedback system will be given, followed by an analysis of the stability and temporal characteristics of a simple voltage–clamp circuit. Finally, after a short review of the many different membrane-clamp systems developed since the invention of the voltage clamp technique, and having identifyed the important characteristics of a membrane with respect to the clamp attainment, an estimate of the value of these parameters will be given in the case of the *Xenopus* oocytes.

3.2 Principles of operation of the voltage clamp

To voltage clamp means that the membrane potential is forced to be constant locally across a piece of membrane; this is done with a negative feedback electronic circuit which in the meanwhile measures the current

flowing through the same piece of membrane. For the interpretation of the current measurements it is critically important that the measured current is only coming from the clamped membrane: in other words, all the membrane surface contributing to the current should be equipotential.

Two problems have to be resolved in order to control the membrane potential V_m. The first is a *spatial* problem, called also the space clamp problem (see Taylor et al., 1960; Chandler et al., 1962): how to obtain uniformity of V_m along the entire piece of membrane of interest?

The second problem is a *temporal* one: for a good clamp of V_m rapidity and fidelity of clamping are essential, the two variables being strictly interconnected, as will be explained later.

We shall analyze in the rest of this section the main aspects of the temporal problem.

Rapidity is needed because, if we want to obtain a clear separation of the capacitative current from the ionic current (see section 3.1) the potential across the membrane following a given step change in the command should have non–zero time derivative only for a time much shorter than the time needed for ionic excitation to develop. Before the development of time–dependent ionic currents, in fact, the membrane current is composed only of a possible steady conductance component summed up with the capacitative current. This latter thus masks only a component of the ionic resistive current (called leak current) which usually is not the object of interest, and moreover can be measured otherwise. But if the ionic time–dependent conductances under study develop in a time shorter than the clamp rise time, the isolation of this time–dependent current is impossible.

Fidelity of clamping is also very important, to be sure that one is separating time– from voltage–dependence of an ionic current. The lack of fidelity, with the membrane potential only approximately following the command value, can invalidate the measurements of a voltage–dependent kinetics. A good fidelity level can be difficult to obtain for various reasons. For example, a high gain in the feedback circuit is necessary for fidelity

(see section 3.2.6), but it can happen that instability or oscillations arise while increasing the gain. Another problem could arise if, during membrane excitation a big amount of current needs to pass through the membrane to clamp the potential: then an insufficient power stage in the electronic circuit (see below) could be unable to provide all the current needed.

For full accounts on the voltage clamp technique theory and first applications see Moore and Cole (1963); Moore (1971); Cole (1972).

*3.2.1. Feedback systems..*A voltage clamp system is an example of a feedback system: this is a system whose general purpose is to fix to an externally supplied value (constant or variable) a measurable quantity characteristic of the system (that we will call q_{reg}, the regulated quantity).

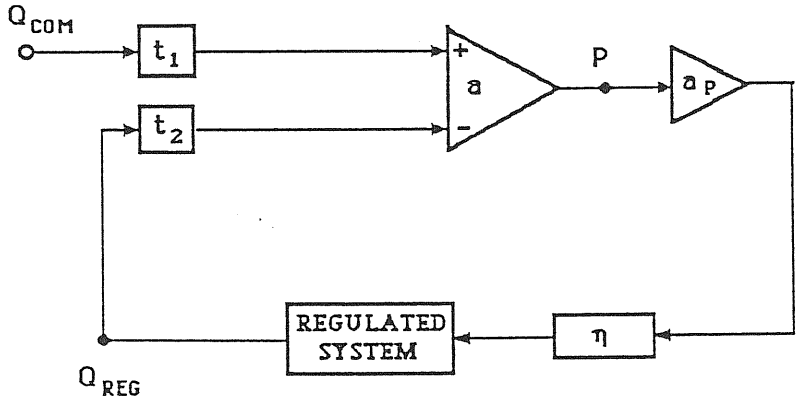

Fig. 3.2. General scheme of a one–loop feedback system (note that this is not in general an electrical circuit, because of the transduction steps). Here t_1, t_2 are the transducers of the command signal and of the q_{reg} respectively. a is the differential amplifier and a_p is a power stage, i.e. an amplifier with a high voltage power supply for injection of the required power in the feedback loop. η stands for an effector system (ex.g. the micropipette).

The operational principle is based on the following procedure: the q_{reg} is measured, (transduced to an electric voltage, if it is not) and compared continually with the command quantity, q_{com}. The error, that is to say the difference signal, is utilized to automatically vary the q_{reg} in the direction of the error cancellation. The general scheme of a feedback system is indicated in fig. 3.2 for the simple case of a one–loop feedback system.

We shall consider hereon the case of an electrical system, where q_{reg} and q_{com} are the voltages v_{reg} and v_{com}, so that the transducers do not exist.

We shall call $A(s), A_p(s), \eta(s)$ the transfer functions of the amplifiers a, a_p (see fig. 3.2) and of the effector η. The Laplace transforms [1] of a generic time–dependent function $f(t)$ will be noted $F(s)$.

*3.2.2. Open loop gain..*The definition of the open loop gain g_{loop} is useful for an almost immediate recovery of the system input–output relations and transfer function [2] (in the approximation of linear electrical behaviour for

---

[1] "The Laplace transformation L associates a unique function $F(s)$ of a complex variable s with each suitable function $f(t)$ of a real variable t. This correspondence is essentially reciprocal one–to–one for most practical purposes; corresponding pairs of functions $f(t)$ and $F(s)$ can often be found by reference to tables. The Laplace transformation is defined so that many relations between, and operations on, the functions $f(t)$ correspond to simpler relations between, and operations on, the functions $F(s)$. This applies particularly to the solution of differential and integral equations. It is, thus, often useful to transform a given problem involving functions $f(t)$ into an equivalent problem expressed in terms of the associated Laplace transforms $F(s)$". From 'Mathematical Handbook', Korn A.G. and Korn T.M. (1965). See Korn and Korn, op. cit., for a short precise on the Laplace transformation.

[2] A transfer function $T(s)$ can be defined for the unknown solution $x(t)$ of any linear ordinary differential equation of the type

$$a_n \frac{d^n x(t)}{dt^n} + a_{n-1} \frac{d^{n-1} x(t)}{dt^{n-1}} + \cdots + a_1 \frac{dx(t)}{dt} + a_0 = f(t) \quad .$$

$T(s)$ is the Laplace transform of the solution $\bar{x}(t)$ corresponding to $f(t)=\delta(t)$ and to the initial condition $x^{(i)}(0)=0$, $i=1,\cdots,n$ with $x^{(i)}=d^i x/dt^i, x^{(0)}=x$. This condition can be translated by saying that the forcing function $f(t)$ is an impulse given at time 0 (represented by the δ function), and the solution and its derivative up to n–th order are 0 at time 0, i.e. the system is at rest before the impulsive stimulation at time 0. It follows from the properties of the Laplace transforms that the solution $x(t)$ for a generic forcing function $f(t)$, and the same initial conditions as above, is obtained, in the transform's domain, by the product $T(s) \cdot F(s)$, where $F(s)=L(f)(s)$; this product corresponds to the convolution of $\bar{x}(t)$ with $f(t)$. Due to this property the transfer function is a very useful concept simplifying the task of predicting the response of the solution of any linear equation to an arbitrary forcing function. The transfer function is thus largely utilized in the study of linear electrical circuits (see Bertolaccini et al.,

the system) and for the study of the system stability.

Suppose to give a nul command signal, so that the positive input to the differential amplifier is 0; and suppose to cut the loop in fig. 3.2 at any point, for example at point P.

Then, if an input test signal $v_i(t)$ is injected at the right hand side of the cut in P, the output signal at the left hand side of the cut, $v_o(t)$, is related to $v_i(t)$, in the Laplace transform domain, by

$$V_o(s) = G_{loop}(s)\ V_i(s)$$

where

$$G_{loop}\ (s) = -A(s)A_p(s)\eta(s)$$

is the transfer function of the indicated open loop.

Now suppose that the loop is closed at P and an input signal $v_{com}\ (t)$ is given to the positive input of the differential amplifier. Then the output of the differential amplifier $V_o(s)$ is

$$\begin{aligned} V_o(s) &= A(s)\left[V_{com}(s) - V_{reg}(s)\right] \\ &= \left(AV_{com} + V_oG_{loop}\right)(s) \end{aligned}$$

because $-AV_{reg} = V_oG_{loop}$; and

$$V_o(s) = V_{com}(s)\frac{A(s)}{1 - G_{loop}(s)}$$

so that

$$V_{reg}(s) = V_o(s)A_p(s)\eta(s) = \frac{A(s)A_p(s)\eta(s)}{1 - G_{loop}(s)}\ V_{com}\ . \qquad (3.1)$$

Generally speaking, one can say that if a signal is injected at any point in the loop, the output signal transform after passing through n elements in the loop will be the input signal, times $1/(1 - G_{loop})$, times the product of the transfer functions of the elements between the input and output points, as is exemplified above (eq. 3.1) for input at a_+ and output at the regulated system's output.

1975).

*3.2.3. Voltage regulator with capacitative load: the voltage clamp.*To see how we can use the G_{loop} concept for a study of the response, stability and oscillations of a given system, we shall apply the above formulas to a voltage regulator, that is a feedback system where the regulated system is an electrical load with impedence Z_l, given by the parallel of a resistance R_l and a capacitance C_l : $Z_l = R_l/(1+sR_lC_l)$; V_{reg} is the voltage at one pole of the load with respect to earth at the other pole. The effector η is a resistance R (see fig. 3.3).

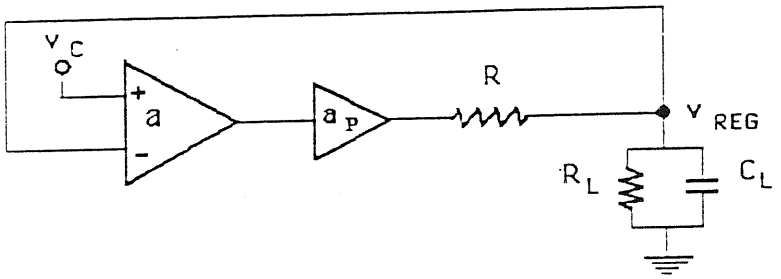

Fig. 3.3. A voltage regulator with capacitative load.

Usually, in the simpler case, an amplifier is characterised by a transfer function of the following type:

$$A(s) = \frac{A}{1+s\tau}$$

which is the transfer function for a simple low–pass filter with cut–off frequency $1/\tau$.

So, assuming a cut–off frequency $1/\tau$ for a and $1/\tau_p$ for A_p, the open loop gain of the voltage regulator is

$$G_{loop}(s) = -A(s)A_p(s)\frac{Z_l(s)}{Z_l(s)+R}$$

where the last factor is the gain factor for a voltage divider with impedances R and Z_l. Substituting the expressions for $A(s)$ and $A_p(s)$,

$$G_{loop} = -AA_p\frac{R_l}{R+R_l}\ \frac{1}{1+s\tau}\ \frac{1}{1+s\tau_p}\ \frac{1}{1+s\frac{R_l\tau_l}{R+R_l}} \qquad (3.2)$$

with $\tau_l = R_l C_l$. By applying the formulas of the last section we can now express V_{reg} as a function of V_{com} :

$$V_{reg}(s) = T(s) V_{com}(s) \quad ,$$

$$T(s) \equiv \frac{A(s) A_p(s) \frac{Z_l(s)}{Z_l(s)+R}}{1 - G_{loop}(s)}$$

$$= \frac{A A_p \frac{R_l}{R+R_l} \frac{1}{1+s\tau} \frac{1}{1+s\tau_p} \frac{1}{1+s\frac{R_l \tau_l}{R+R_l}}}{1 + A A_p \frac{R_l}{R+R_l} \frac{1}{1+s\tau} \frac{1}{1+s\tau_p} \frac{1}{1+s\frac{R_l \tau_l}{R+R_l}}} \quad .$$

If we suppose that the command input can be a time dependent function the above formulae apply to a voltage clamped passive linear membrane (because in a passive linear membrane, by definition, Z_l is constant with time and voltage). If we identify the R element with the current microelectrode, for example, this could be a scheme of a microelectrode clamp.

From a study of the transfer function $T(s)$ we can now derive information on the stability of the feedback loop and on the time–dependent properties of the stable cases (in particular on the rapidity and fidelity of the response v_{reg}).

*3.2.4. Stability as a function of the gain.*A system's transfer function $T(s)$ is a complex function of the complex variable s, and in normal cases it reduces to a ratio of polinomials.

The system response will be stable for a finite input if all the $T(s)$'s poles [1] in the complex plane have negative real part. This property ensures that the response will depend upon time through a sum of exponential terms with negative coefficients of the exponents, so that the time evolution will be a sum of relaxations towards a finite value. If one pole, moreover, happen to have non–zero imaginary component, than the corresponding exponential term in the response will be multiplied by an oscillating factor.

(1) The poles of a function of a complex variable are its singularities in the complex plane.

In the case of our voltage regulator, the poles of $T(s)$ will be the poles of $G_{loop}(s)$ plus the zeros of the expression $1 - G_{loop}(s)$. $G_{loop}(s)$ has here three poles with negative real part,

$$p_1 = -\frac{1}{\tau}$$
$$p_2 = -\frac{1}{\tau_p}$$
$$p_3 = -\frac{R + R_l}{R_l \tau_l}$$

It can be seen from eq. 3.2 that the zeros of $1 - G_{loop}(s)$ are the solutions of the algebraic equation of third order $1 - G_{loop}(s) = 0$. In fact if we write

$$G_{loop}(s) = -\alpha \frac{1}{\prod_i (s - p_i)} \equiv -\alpha \frac{N(s)}{D(s)} \qquad (3.3)$$
$$\alpha \equiv A A_p \frac{R_l}{R + R_l}$$

than the algebraic equation is $D(s) + \alpha N(s) = 0$. We shall find qualitatively the behaviour of the real part of the three solutions, as a function of the parameter α, i.e. of the gain AA_p. This is reasonable because in a voltage clamp system the gain is usually under control of the experimenter. For $\alpha = 0$ (zero gain) the poles of $T(s)$ are the poles of G_{loop} reported above. For $\alpha \rightarrow \infty$ the poles of $T(s)$ become the zeros of G_{loop} ; here they are at infinity. With α varying from 0 to ∞, the poles move from the p_i, which lie on the negative real axis, towards ∞, along three curves that asintotically coincide with the three straight lines of slope given by

$$\varphi_n = \frac{\pi}{3} \pm \frac{2}{3} n\pi = \{60^o, 180^o, 300^o\} \quad (n = 0, 1, 2).$$

This result is obtained applying the constraints $G_{loop} = 1$ and $arg\,[-G_{loop}] = \pi \pm 2n\pi$, deriving from $1 - G_{loop} = 0$, and observing that from eq. 3.3 follows

$$arg\,[-G_{loop}] = \sum_i arg(s - p_i) + arg(\alpha) = \sum_i arg(s - p_i)$$

so that

$$arg\,[-G_{loop}] \Rightarrow \quad 3\varphi$$

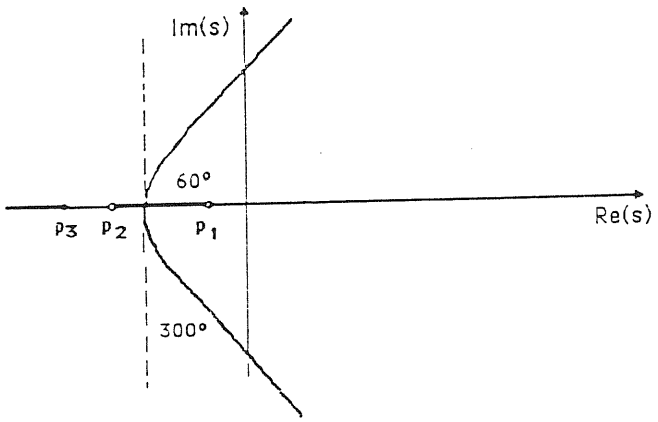

Fig. 3.4. The locus of the poles, in the complex plane, of the transfer function $T(s)$ of the voltage regulator of figure 3.3 (see text).

when s tends to the n–th zero of G_{loop} laying at ∞. The locus of the poles of $T(s)$ when the gain varies is drawn in fig 3.4.

We see that for high gain the system has poles with positive real part, corresponding to instability; for intermediate values of the gain α, the system is stable but it oscillates, because the imaginary part of the poles is non zero. So the voltage regulator with three simple poles in the open loop gain can present instability (as does any system whose transfer function has more than two simple poles), and it can display damped oscillations.

In a voltage clamp circuit using microelectrodes, there are always (unwanted) capacitative couplings between different branches resulting in additive time constants (poles in $T(s)$), so that instability is always possible as the gain is modified; and this in the practice causes saturation of the instrumentation.

*3.2.5. The clamp of a non linear excitable membrane. Rapidity of the clamp.*We talked extensively about the system in fig. 3.3 because, as was said above, this is a good and simple model of a clamped passive membrane; and moreover, the linearized equations for a non linear membrane model can be studied in the proximity of a stable point by the Laplace transform method presented above. This was done by G.M. Katz and T.L. Schwartz (1974). They have shown that, for a clamped membrane modeled with a

circuit differing from the one presented above for the presence of only one instrumental time constant and for a parallel time– and voltage–dependent conductance added to the passive membrane resistance R_m (see fig. 3.5), the equations for the non linear evolution of the membrane potential v_m are:

$$\begin{aligned}\frac{d^2v_m}{dt^2} &+ \left\{\frac{1}{\tau_e}+\frac{1}{\tau_m}+\frac{1}{\tau}+\frac{1}{\tau_s}\right\}\frac{dv_m}{dt} \\ &+ \left\{\left(\frac{1}{\tau_e}+\frac{1}{\tau_m}+\frac{K+1}{\tau_s}\right)\frac{1}{\tau}+\frac{d}{dt}\left(\frac{1}{\tau_e}\right)\right\}v_m \\ &= \frac{K}{\tau\tau_s}v_{com}+\left\{\frac{1}{\tau\tau_e}+\frac{d}{dt}\left(\frac{1}{\tau_e}\right)\right\}E.\end{aligned} \tag{3.4}$$

where the parameters appearing in the equations are defined as in fig. 3.5: K is the differential amplifier gain, $\tau_e = C_m/g(v_m,t)$, $\tau_m = R_mC_m$, $\tau_s = (R_{s1}+R_{s2})C_m$, τ is the instrumental time constant and E is the membrane equivalent electromotive force. We want to stress that here R_s stands for a resistance in series with the current electrode (sometimes called the access resistance), while no resistance in series with the voltage electrodes is considered in this simple system.

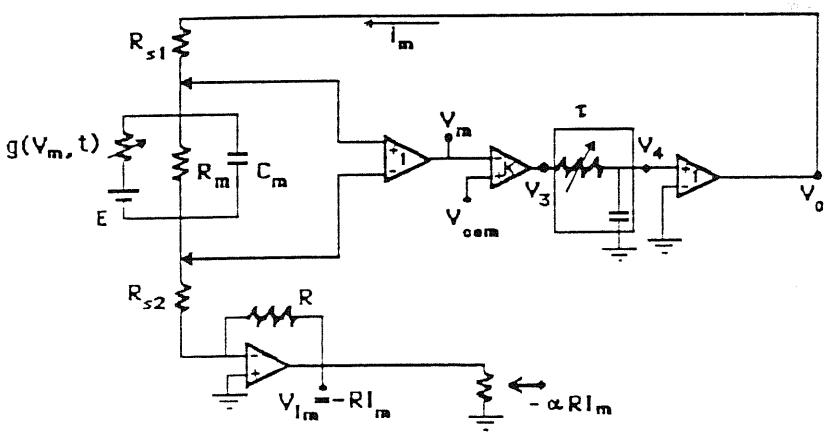

Fig. 3.5. The equivalent circuit for a voltage clamped membrane (from Katz and Schwartz , 1974).

In the rest of this section we shall refer to this circuit. We assume now that the system is in a stable point $[\bar{v},\bar{g}(\bar{v},\infty)]$ for $v_{com} = \bar{v}$, and we set

for simplicity $\bar{v} = 0$. Then the linearization in the proximity of this point is obtained by setting

$$\frac{1}{\tau_e} = 0 \; ; \qquad \frac{d}{dt}\left(\frac{1}{\tau_e}\right) \propto \frac{d}{dt} g = 0 \; .$$

The condition for linearization, $\frac{dg}{dt} = 0$, is generally valid if the variable membrane conductances develop in a time much longer than the time needed for clamping v_m after a step in the command.

With this assumption eq. 3.4 reduces to

$$\frac{d^2 v_m}{dt^2} + \left\{ \frac{1}{\tau_m} + \frac{1}{\tau} + \frac{1}{\tau_s} \right\} \frac{dv_m}{dt} + \left\{ \left(\frac{1}{\tau_m} + \frac{K+1}{\tau_s} \right) \frac{1}{\tau} \right\} v_m = \frac{K}{\tau \tau_s} v_{com} \; . \quad (3.5)$$

The solution $v_m(t)$ is obtained antitrasforming the relation

$$V_m(s) = T(s) V_{com}\ (s)$$

with

$$T(s) = \frac{K}{\tau \tau_s} \frac{1}{(s - p_1)} \frac{1}{(s - p_2)}$$

and

$$p_{1,2} = -\frac{1}{2} \left\{ \frac{1}{\tau_l} + \frac{1}{\tau} \pm \sqrt{\left(\frac{1}{\tau_l} - \frac{1}{\tau} \right)^2 - \frac{4K}{\tau \tau_s}} \right\} .$$

where τ_l is now defined as $\tau_l = \left(\frac{1}{\tau_m} + \frac{1}{\tau_s} \right)^{-1}$. The antitrasformation of the V_m / V_{com} relation for a step change in $v_{com}(t)$ from 0 to V_c is (in the generic case):

$$v_m(t) = V_c \frac{K}{\tau \tau_s} \left\{ \frac{1}{p_1 (p_1 - p_2)} \left[e^{p_1 t} - 1 \right] - \frac{1}{p_2 (p_1 - p_2)} \left[e^{p_2 t} - 1 \right] \right\} .$$

Thus $v_m(t)$ relaxes to the stable value

$$V_c \frac{K}{\tau \tau_s} \frac{1}{\tau \tau_l + \frac{K}{\tau \tau_s}} = V_c \frac{\beta K}{1 + \beta K}$$

where $\beta = \tau_l / \tau_s = (R_m / (R_m + R_s))$. The *rapidity* of the clamp is limited by $1/Re(p_1) = 1/Re(p_2) = -\frac{1}{2}(\frac{1}{\tau_l} + \frac{1}{\tau})$. This is the time interval which should be much shorter than the time needed for membrane conductance

changes. With the approximation introduced by Katz and Schwartz of an infinite bandwidth for the power stage a_p, there are only two time constants, corresponding to two poles in G_{loop} , and there is no instability in the loop for any gain a, in contrast with the general case with three or more poles. But oscillations are still possible, when $Im(p_1) = Im(p_2) \neq 0$. Oscillations must generally be avoided, because they disturb the observation of the onset of excitation. In order to obtain the maximum fidelity at steady state of the v_m value to V_c, the clamp conditions of gain and frequency response are usually adjusted to the highest possible gain value that do not generate oscillations: this is called the critical damping condition. In the simple model of Katz and Schwartz the critical damping and overdamping correspond, respectively, to to

$$\frac{4K}{\tau\tau_s} \leq \left(\frac{1}{\tau_l} - \frac{1}{\tau}\right)^2 \quad . \quad . \tag{3.6}$$

The authors analyze in their paper the extreme cases when

$\tau_l \gg \tau$ (slow membrane–solution load with respect to fast clamp)

$\tau \gg \tau_l$ (slow clamp with respect to fast load).

These conditions are in fact expression of the requirement of a high gain K (high fidelity), for which a high value of the difference $\frac{1}{\tau_l} - \frac{1}{\tau}$ is needed. It is always preferable to obtain one of these two cases in the practice.

Katz and Schwartz analyze, in the case of critical damping, the 'slow clamp' and the 'fast clamp' cases. They obtain a numerical value for the time needed to the membrane to reach 90% of its final potential value (*rapidity* of the clamp circuit):

$$t_{90} = 7.78\ \tau \qquad (fast\ \ clamp)$$
$$t_{90} = 7.78\ \tau_l \qquad (slow\ \ clamp)$$

They also show that, in the case in which neither a 'fast' nor a 'slow' clamp can be realised, and as a consequence the rapidity t_{90} of the clamp is scarce, it is possible to solve the problem by means of a new feedback injection of a fraction of the membrane current into point A (current is added to the error signal $V_{com} - V_m$); this technique reduces τ_s, and speeds up the clamp

(even if the effect of R_s –the series resistance– cannot be completely canceled because this resistance consists in reality of a complex impedance).

3.2.6 Fidelity of the clamp. Finally, Katz and Schwartz study the fidelity of their clamp, i.e. the fidelity of the steady state value of v_m to the command voltage value. If a membrane is passive (linear) than v_m/V_c at steady state is given by $T(0)$, the zero–frequency transfer function: this latter equals $\beta K/(1+\beta K)$, and it approaches 1 (its maximum) as the gain K increases, and as R_s, the series resistance, decreases (β increases). Consequently, as is stressed by Smith et al. (Smith et al., 1980), it is important to have a low value of R_s, the lowest compatible with a stable recording and with the need to avoid injury of the cell.

However normally a biological membrane is not linear, and from eq. 3.2.1 one sees that

$$v_m = \frac{v_{com} + \frac{\tau\tau_s}{K}\left\{\left[\frac{1}{\tau\tau_e} + \frac{d}{dt}\left(\frac{1}{\tau_e}\right)\right] - \frac{d^2 v_m}{dt^2} - \left[\frac{1}{\tau_e} + \frac{1}{\tau_m} + \frac{1}{\tau} + \frac{1}{\tau_s}\right]\frac{dv_m}{dt}\right\}}{\frac{\tau\tau_s}{K}\left\{\left(\frac{1}{\tau_e} + \frac{1}{\tau_m} + \frac{K+1}{\tau_s}\right)\frac{1}{\tau} + \frac{d}{dt}\left(\frac{1}{\tau_e}\right)\right\}}.$$

In the case of a 'fast clamp' the limits $\tau_l \gg \tau$ and $K \gg 1$, together with the critical damping condition (3.6), give $v_m \approx V_c$, and the fidelity of the clamp in this limit is independent of the membrane–electrode load, and so it is not dramatically influenced, for example, by excitation: a 'fast clamp' can excellently clamp a spike. In the case of 'slow clamp' instead, the effect of a variable membrane conductance is dramatic, and the more rapid are the variations of g, the more v_m is degradated. Therefore a 'slow clamp' is good for studying slow changes in membrane conductance, or steady–state current fluctuations.

It must be said that real voltage clamp systems are usually more complicated than the one studied above; they have many instrumental time constants, they can be unstable, and the definitions of 'slow' and 'fast' clamp given above are not immediately applicable; but these definitions have to be kept in mind as a clarifying description and a sometimes useful approximation.

Cell	$\tau_m = R_M C_M$ (sec)	$\tau_S = R_S C_M$ (sec)	$\tau_L = \frac{\tau_i \tau_S}{\tau_i + \tau_S}$ (sec)	β	K	τ (for critical damping) (sec)	
						$\tau_L \gg \tau$	$\tau \gg \tau_L$
Squid axon (1)	1.25×10^{-3}	6.3×10^{-6}	6.3×10^{-6}	1	200 to 1,000	7.9×10^{-9} to 1.6×10^{-9}	5.0×10^{-3} to 25.0×10^{-3}
Eel electroplaque (2)	114×10^{-6}	100×10^{-6}	53×10^{-6}	0.53	1,300	19.2×10^{-9}	140×10^{-3}
Puffer supramedullary ganglion cells (3)	5×10^{-3}	85×10^{-3}	4.7×10^{-3}	0.057	5,000	4.1×10^{-6}	5.4

Calculations were made from data in (1) Cole & Moore (1960), (2) Nakamura *et al.* (1965) and Schwartz *(unpublished)*, and (3) Hagiwara & Saito (1959).

(1) 0.1-cm^2 membrane in central chamber.

(2) 0.05-cm^2 "window".

(3) 200-μ cell.

(1) Cole, K.S. and Moore, J.W. (1960). 'Ionic current measurements in the squid giant axon membrane'. Biophys. J. 2:105.

(2) Nakamura, Y., Nakajima, S. and Grunfest, H. (1968). 'Analysis of spike electrogenesis and depolarizing K inactivation in the electroplaque of *Electrophorus electricus*, L'. J. Gen. Physiol. 49:321.

(3) Hagiwara, S. and Saito, N. (1959). 'Membrane potential change and membrane current in supramedullary nerve cell of puffer'. J. Neurophysiol. 22:204.

Table 3.1 Approximate resting membrane parameters for three types of voltage–clamped preparations (reproduced from G.M. Katz and T.L. Schwartz (1974)).

The exact evaluation of the rapidity of a clamp must be sought in each case; the clamp fidelity for passive membranes can be recovered from $\beta K/(1+\beta K)$, by substituing to K the equivalent zero–frequency gain of the voltage clamp amplifier. It is generally valid that: a) the highest fidelity is obtained with the highest gain; b) if the gain value, for fixed values of the instrumental time constants, is raised enough, the system goes into oscillations ('ringing'), so that there exists an upper optimal value for the gain to achieve critical damping and good fidelity; and c) the minimum R_s/R_m ratio must be sought.

In table (3.1) are shown, for a few preparations, the values of preparation and instrumentation variables and parameters important for obtaining critical damping.

3.3 Special voltage clamp systems

It was said before that different clamp systems have been developed through the years, as the voltage clamp was applied to different kinds of cells. They are described in the book by Hille (1984), with many references to the original papers. Most, but not all methods (see the patch–clamp method) have a feedback amplifier which receives a signal from a voltage recording electrode and compares it with a command potential. The difference is amplified and a current proportional to this difference is applied to the membrane through a current electrode. In chapter 4 a more detailed illustration is given for the case of a double–microelectrode clamp.

Among the various voltage clamp methods we mention (see fig. 3.6):

a) the axial wire methods, to clamp giant axons; here the long wires provide the spatial uniformity of the clamp (see Hodgkin et al., 1952; Cole and Moore, 1960; Chandler and Meves, 1965).

b) the gap methods, used to clamp elongated preparations with small diameters of the fibers, as myelinated and unmyelinated axons and vertebrate muscles fibers (Nonner, 1969; Hille and Campbell, 1976). The vaselin or sucrose gaps provide insulation of a part of the membrane, and permit the spatial isopotentiality.

c) the microelectrode clamps, with one, two or three intracellular microelectodes (see Adrian et al., 1970; Smith et al., 1980; Finkel and Redman, 1984). The technique is mostly used for cells approximately spherical, so to avoid the spatial problem. The presence of the microelectrodes results in a fairly high access resistance in the current injection path. The clamp realised in our work belongs to this category of systems.

d) the suction pipette methods. They use a big–tipped pipette (up to 50 μm in diameter) used to measure potential and pass current. These methods have been used with dissociated cells as cardiac myocytes and neurons, providing perfusion of the interior of the cell as well as voltage clamp (Byerly and Hagiwara, 1982; Kostyuk and Krishtal, 1984).

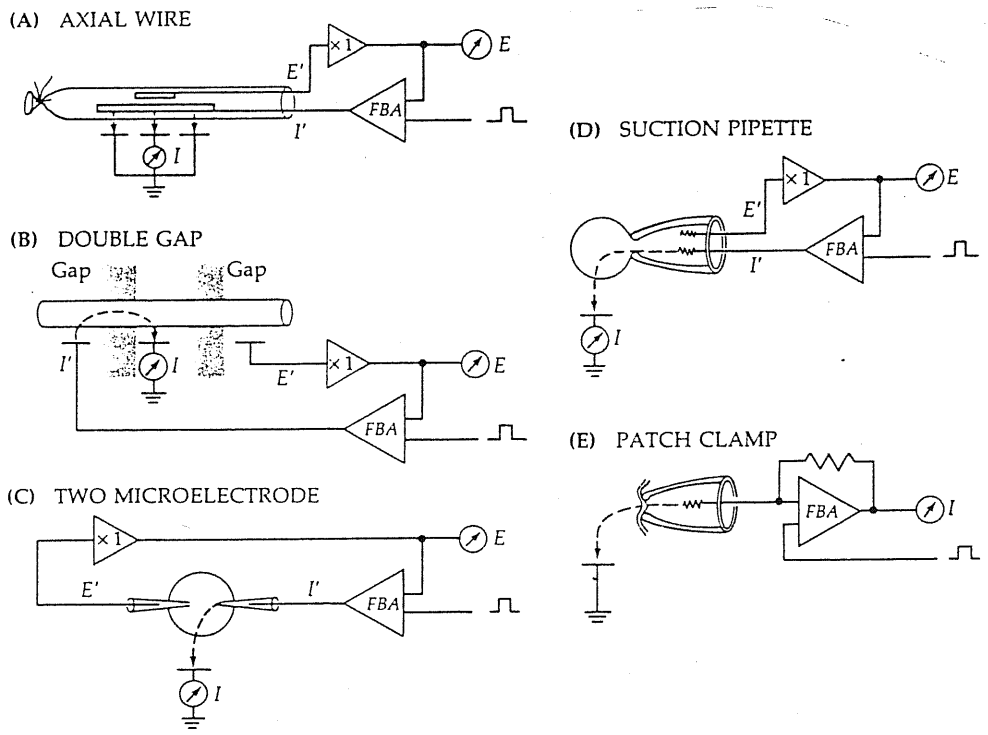

Fig. 3.6: Voltage clamp techniques (from Hille, 1984).

e) the patch clamp method, which uses a single small–tipped pipette (diameter of $\sim$ 1 μm) and a single operational amplifier (a current to voltage–converter) for potential measurement and current injection. The patch clamp can be used, in the case of small cells, (diameter up to a few microns) like a suction pipette method; however it can also be used to record from cell–attached or cell–free patches of membrane. This latter method has permitted the recording of the activity of single membrane channels (see Hamill et al., 1981; Sakmann and Neher, 1983).

*3.3.1. Requirements to clamp Xenopus oocytes..*To understand which kind of

clamp circuit has to be used for a voltage–clamp study of a given preparation in the first place one must have a rough idea of

1) the kinetics of excitation for the membrane under study: this determines the clamp rapidity required;

2) the geometry of the cell to be clamped, and consequently the method that gives the best space clamp.

In the case of *Xenopus* oocytes, as far as the second point is concerned, the two–microelectrodes voltage clamp has generally been applied (see Kusano et al., 1977; Sumikawa et al., 1989), as the oocyte does not present space clamp problems because of its spherical symmetry.

For what concerns the first point, the native *Xenopus* membrane, as is well known, is not very excitable, because the native density of membrane channels is not very high; moreover the membrane conductance variations are slow. All the recorded transmitter–operated currents, for example, develop in times of the order of seconds or minutes (Miledi et al., 1989). So, if one needs to clamp a native oocyte, a slow clamp (here in the sense of a slow response of membrane voltage to the command input) is a good system.

When foreign membrane channels with a fast kinetics are expressed into the oocyte, if one wants to observe the cell membrane currents through the two microelectrodes clamp system, this system should have a fast response. But what is usually done is to separate the two operations of clamping the whole oocyte and measuring the induced membrane activity. The latter operation is performed through a patch–clamp pipette, connected to an independent patch–clamp amplifier (see fig. 3.7), so that a fast voltage clamp is not needed.

For what concerns the oocyte characteristics of importance for the design of the voltage clamp amplifier, the oocyte membrane should usually present an input resistance (the resistance R_m in paragraph 3.2) variable between $100K\Omega$ and $3M\Omega$, with a mean of $0.7M\Omega$, and a capacitance of 6.3 μF for an average egg diameter of 1.14 mm (Kusano et al., 1982). This corresponds, with an average oocyte surface of 0.16 cm^2 to a specific capacitance of $\sim$

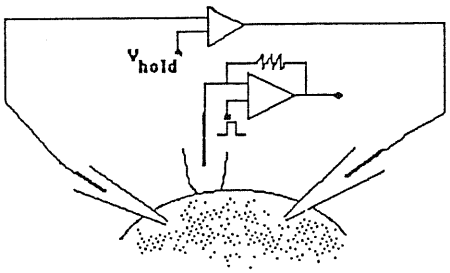

Fig. 3.7. The arrangement for patch–clamping a voltage–clamped oocyte.

39 $\mu F/cm^2$; a second C_m estimate of 11.9 ± 4.3 $\mu F/cm^2$ has been given by Kado et al., (1981). These values of membrane capacitance are high if compared with the normally found value of ~ 1 $\mu F/cm^2$; this is explained with the hypothesis, supported also by morphological data, of a high number of convolutions (microvilli) in the oocyte's membrane, so that the oocyte surface is underestimated when assuming a spherical shape.

If we assume a value of 1 $\mu F/cm^2$, and keeping in mind that usually the current microelectrode access resistance (R_{s1}) can be set to $200 - 500k\Omega$ (see for example Methfessel et al., 1986), then we obtain

$$\tau_m = R_m C_m = 0.7 \ sec$$

$$\tau_s = R_s C_m = 0.5 \ sec$$

$$\tau_l = \frac{\tau_m \tau_s}{\tau_m + \tau_s} = 0.29 \ sec$$

$$\beta = \frac{R_m}{R_m + R_s} = 0.58$$

so that it should be easy to obtain a 'fast' clamp (in the sense of Katz and Schwarz), with a rapidity of let's say a few milliseconds. We shall see in chapter 4 the results obtained with our voltage clamp system.

Chapter 4

Construction of a voltage clamp amplifier

A voltage clamp system consists of a membrane potential preamplifier connected to the voltage clamp amplifier itself. The design and the construction of a double–microelectrode voltage clamp system will be described in this chapter. The design of our voltage clamp amplifier was based on the circuit scheme suggested by Halliwell et al. (1987). The system is intended for use with large, spherical cells, and is suitable for *Xenopus* oocytes. Thus, it was named VCX0, an acronym of 'Voltage Clamp amplifier for *Xenopus* Oocytes.

4.1 The design of a double–microelectrode voltage clamp system.

Before to illustrate in detail the design of our circuit, we shall comment on the schematic arrangement of a generic double–microelectrode voltage clamp system. The scheme is shown in fig. 4.1.

To record the membrane potential, a glass micropipette filled with an electrolitic solution enters the cell. The pipette filling solution is in contact with an Ag/AgCl reversible and non polarizable electrode connected to a voltage preamplifier (more details about the electrodes are given in section 5.5). The intracellular voltage is measured with respect to the bath voltage, which is measured through a second Ag/AgCl electrode ('reference electrode') and an agar bridge. The preamplifier allows the monitoring of the membrane potential and at the same time it works as a voltage follower. This means

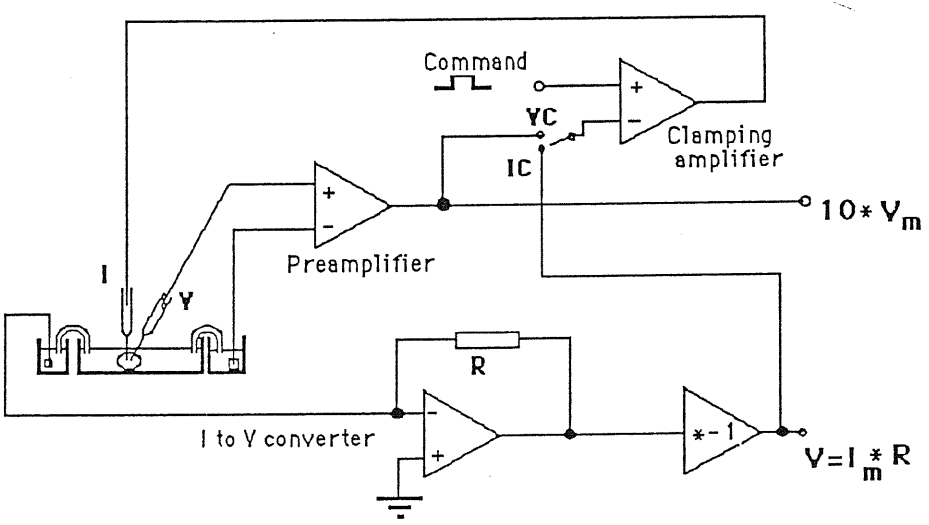

Fig. 4.1: A double–microelectrode voltage clamp.

that the input voltage will be transmitted to the output independently of the load (represented by the monitor, clamp circuit etc.) impedance. This can be obtained due to the very high input impedance of the preamplifier itself, that simulates an open circuit and prevents the flow of current into the preamplifier, and consequently impedes voltage drops along the line preceding the input to the instrument; at the same time, the preamplifier presents a very low output impedance to the following load circuit, so as to simulate a perfect voltage generator, with no voltage drops due to the generator's internal resistance.

The output of the voltage preamplifier is connected to the negative input of the clamping amplifier (a differential amplifier) that subtracts it from the command signal supplied at its positive input, and amplifies the difference voltage with variable gain and frequency response. The output of the clamping amplifier is connected to a current–injecting electrode (an Ag/AgCl electrode in a solution–filled micropipette) inserted in the cell.

The injected current, corresponding to the membrane current, is measured via a bath electrode which offers to the current a path to ground.

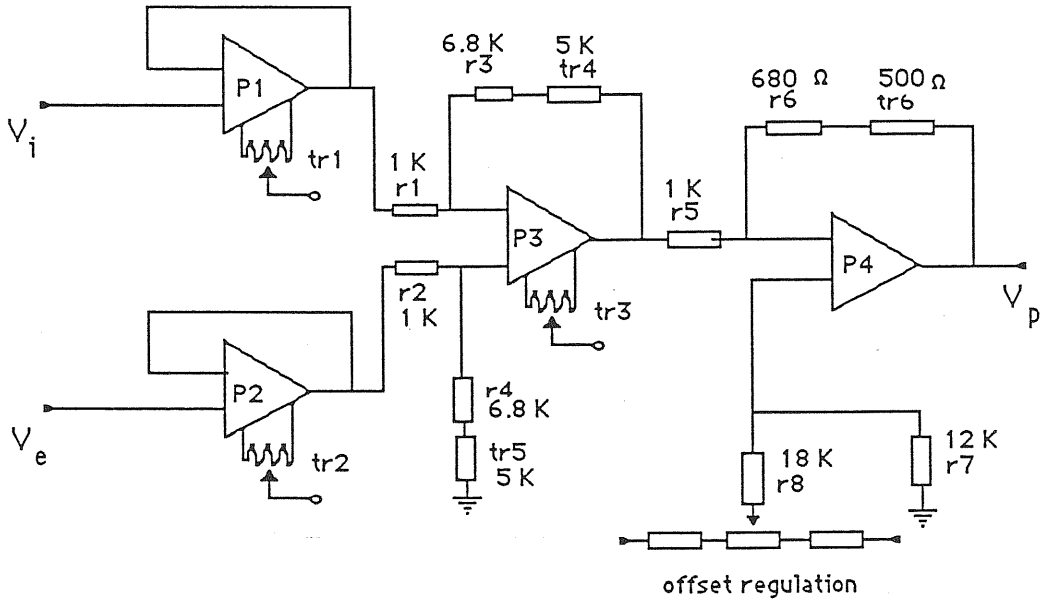

Fig. 4.2: Scheme of the voltage preamplifier used in the voltage clamp system VCX0. For reference to the components used, see section 4.3.

The electrode is in fact an Ag/AgCl electrode in connection with the bath through an agar bridge, and connected to ground through an operational amplifier (opamp) which holds the input (the bath) at earth. It is usually said that the operational amplifier holds the input at 'virtual ground'. The second function of the virtual ground operational amplifier is to convert the current to a voltage, with an optionally adjustable gain, so as to have a good amplification. The signal is then monitored and offers a measurement of I_m, the membrane current. If a series resistance compensation mechanism is added to the system, the voltage output from the current–to–voltage converter, corresponding to $-I_m R$, (see fig. 4.1) is partially fed to the positive input of the clamping amplifier through a potentiometer.

We shall now turn to the details of our circuit. All the components used for the circuit will be specified in section 4.3.

The voltage preamplifier is a differential amplifier (measuring $V_{internal} - V_{bath}$) with a gain of 10. The design of the preamplifier is given in fig. 4.2.

The internal and external signals are passed through the voltage followers $P1, P2$ and fed to $P3$. $P1$ and $P2$ are operational amplifiers in the voltage follower configuration, and they are chosen so as to have a very high ($10^{12}\Omega$) input resistance. $P3$ is an operational amplifier in the differential amplifier configuration, with gain 10 and output $-(V_{internal} - V_{external})$. It is crucial for a good time-response of the preamplifier that the chip for $P3$ is able to make a very fast comparation between its positive and negative input. Thus it must have a very fast frequency response: here the time required for the error voltage, i.e. the voltage at the inverting input of the amplifier, to settle to within 0.01% of its final value from the time a 10 V step input is applied to the inverter, is 1.5 μsec (see Linear Databook, NSC). The difference signal $-(V_{internal} - V_{external})$ goes to the negative input of $P4$, in the differential configuration, with gain 1. $P4$ receives at its positive input an offset signal. The possibility to add an offset signal to the measurement is needed to compensate for eventual voltage drops as those produced at the electrodes–solution interface, or due to liquid junction potentials. The aim of using more than one operational amplifier is the fine tuning of gain and the rejection of signals common to the two inputs of the preamplifier.

Our voltage clamp amplifier circuit scheme is given in fig. 4.3. The clamping amplifier is the combination of three operational amplifiers, with variable overall gain from 44 to 4400. The frequency response of the amplifier is adjustable by means of a 4–way switch that varies the value of the feedback capacitor of the operational amplifier $A3$ between 10 and 100 nF (10, 22, 50 and 100 nF). $A3$ is the real critical component determining the rapidity of the clamp circuit, and has the same settling time characteristics as P3 (see above). An additional high–voltage output stage (not essential for small cells, or not very excitable cells) is realised with the high voltage operational amplifier $A5$. It allows a gain of 1.35 up to 15, so that finally the system's gain goes from 59 to 66000.

The command signal is fed to $A2$ after having been summed with an offset signal and with the optional signal for the series resistance compensation, and then having been inverted at $A1$ and filtered with a variable low–pass filter. The filter slows the risetime of the command signal: this is

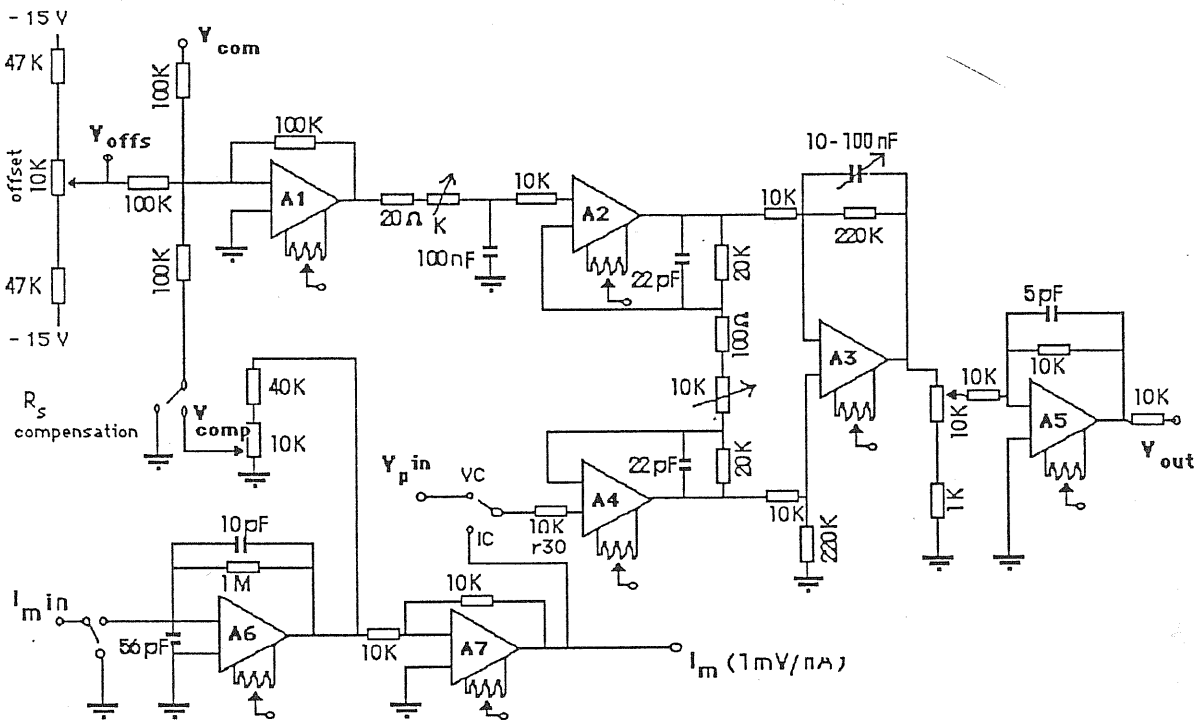

Fig. 4.3: Scheme of the voltage clamp amplifier circuit used for VCX0. For reference to the components used, see section 4.3.

sometimes needed to obtain a voltage clamp step without oscillations. Because of the $\times 10$ gain of the preamplifier and because of the inversion of the command signal at $A1$ the command voltage supplied by the operator must be $-10 \cdot V_{com}$, where V_{com} is the desired potential.

The membrane current is measured through a bath electrode connected to virtual ground through an I–V converter operational amplifier, with a feedback resistance of 1 $M\Omega$. The signal is then passed through an inverting operational amplifier and monitored. The output voltage signal can be converted into a current value by multiplying it by the (fixed) gain factor

of 1 mV/nA.

4.2 The system transfer function

To evaluate the rapidity and fidelity performances of our voltage clamp system, its internal time constants and zero–frequency gain factor must be evaluated. This will be done by writing down the transfer function $T(s)$ (see section 3.2) of the voltage clamp system composed of the preamplifier, the clamping amplifier shown in fig. 4.3, and the membrane–electrode load, considering the membrane a passive R–C system. The whole system is shown in fig. 4.4.

From the final form of $T(s)$ the gain factor of the clamp and the circuit time constants will result. Standard values taken from the literature will be used for R_m and C_m (see section 3.3). The operational amplifiers will be considered as ideal opamps, with infinite open loop gain and infinite bandwidth (zero internal time constants), so that the gain and frequency response for each opamp are settled by the externally supplied components in the amplifier feedback loop.

With these assumptions, we shall construct $T(s)$ by writing the transfer function of separated stages in the circuit, and finally multiplying the results.

The output V_o of an ideal opamp as a function of its positive and negative inputs V_+, V_-, and for a generic configuration of the amplifier as the one shown in fig. 4.5, is

$$V_o = V_+ \frac{Z_2}{Z_1 + Z_2} \frac{Z_3 + Z_4}{Z_3} - V_- \frac{Z_4}{Z_3} \tag{4.1}$$

where the Z_i, $i = 1, \ldots, 4$, are complex impedances. Note that the above relation is a relation between the Laplace transforms of the time–dependent quantities $v_o(t), v_+(t)$, $v_-(t)$. This relation can be obtained by applying the simple Kirchoff's laws to the system in fig. 4.5. The formula (4.1) is useful in writing down the transfer function for each opamp, just substituting to the $Z_i's$ their exact value, and is used throughout the following computations.

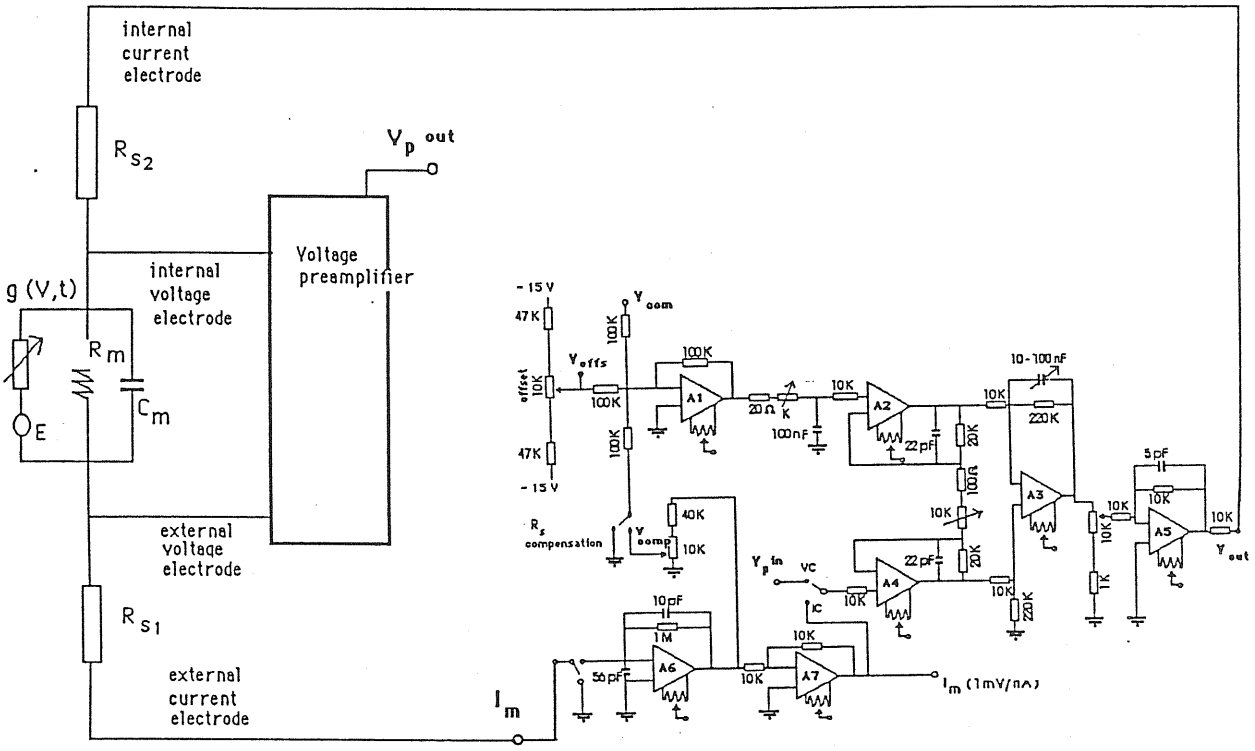

Fig. 4.4: Voltage clamp circuit, including preamplifier, clamping amplifier and membrane–electrode load.

We refer in the following to the nomenclature and to the system's blocks defined in fig. 4.6. We shall give the input–output relation for each block in the Laplace transform's domain (see section 3.2). s is the complex coordinate in that domain.

Block 1): here $A1$ is in the summing amplifier configuration:

$$V_{A1} = -(V_{com} + V_{offs} + V_{comp}) \ .$$

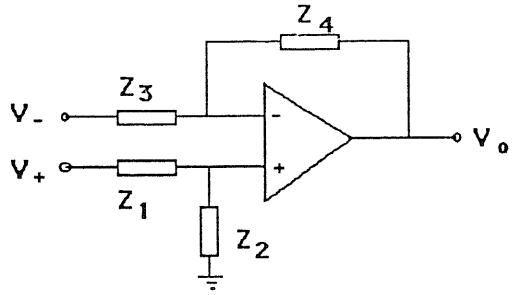

Fig. 4.5: The generic configuration of an operational amplifier.

Block 2) is a low pass filter for the command signal.

$$V_{+1} = V_{A1}\frac{1}{1+s\tau_{filter}}$$
$$\tau_{filter} = R_{filter}\cdot 100\ nF\ \in [10^{-6}sec, 10^{-4}sec]\ .$$

Block 3) is the first part of the main differential amplifier of the clamp.

$$V_{+} = V_p + (V_p - V_{+1})G\frac{1}{1+s\tau_c}$$
$$V_{-} = V_{+1} - (V_p - V_{+1})G\frac{1}{1+s\tau_c}$$

where

$$G \equiv \frac{20K\Omega}{R_{gain}} \in [1.98, 200] \qquad \tau_c = 22\ pF\cdot 20\ K\Omega = 0.44\ \mu sec\ .$$

Block 4) is the central stage of the clamp amplifier.

$$V_{A3} = 22\cdot\frac{1}{1+s\tau_d}[V_{+}(1+s\tau_{+}) - V_{-}]$$

where C varies in the set $\{10\ nF, 22\ nF, 50\ nF, 100\ nF\}$ so that

$$\tau_d \equiv 220K\Omega\cdot C$$
$$\in \{2.2\cdot 10^{-2}sec, 1.1\cdot 10^{-2}sec, 4.8\cdot 10^{-3}sec, 2.2\cdot 10^{-3}sec\}$$

and

$$\tau_{+} \equiv (10K\Omega\cdot 220K\Omega)/(10K\Omega + 220K\Omega)\cdot C$$
$$\in \{9.5\cdot 10^{-5}sec, 2.1\cdot 10^{-4}sec, 4.7\cdot 10^{-4}sec, 9.5\cdot 10^{-4}sec\}\ .$$

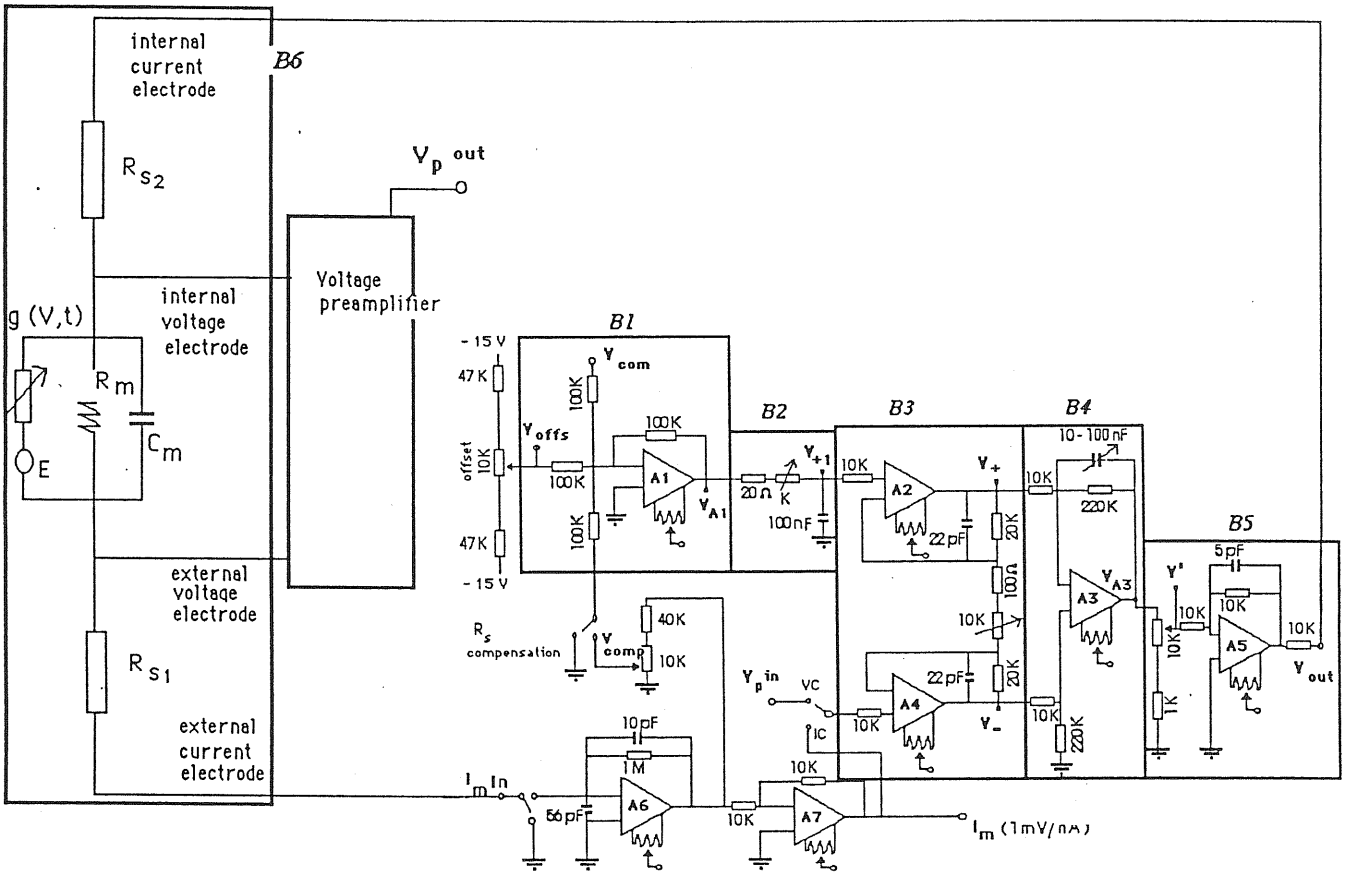

Fig. 4.6: Block subdivision of the voltage clamp system. The different block's input–output relations are used to form the final input–output relation of the system (see text).

Block 5) contains the power stage and the output to the current microelectrode. Here

$$V' = V_{A3}\frac{11K\Omega - R'_{gain}}{11K\Omega} = V_{A3} \cdot G_c$$

so that

$$V_{out} = -V' \cdot 15 \cdot \frac{1}{1 + s\tau_{hv}}$$

$$= -V_{A3} \cdot G_c \cdot 15 \cdot \frac{1}{1 + s\tau_{hv}}$$

where $\tau_{hv} \equiv 150K\Omega \cdot 5.6\,pF = 0.8\,\mu sec$ and $G_c \equiv [(11K\Omega - R'_{gain})/11K\Omega] \in$

$[0.09, 1]$.

Block 6). V_m as a function of the voltage in the current microelectrode (V_{out}) is obtained by applying the rule of the voltage divider:

$$V_m = \frac{Z_m}{Z_m + R_s} V_{out} = \frac{R_m}{R_m + R_s} \cdot \frac{1}{1 + s\tau_m \frac{R_s}{R_s + R_m}}$$

where $R_s \equiv R_{s1} + R_{s2}$ and $\tau_m \equiv R_m C_m$.

Finally, the preamplifier just multiplies its input signal by a gain factor of 10.

We can now write the final form of our transfer function. We first write the open loop gain G_{loop} , by setting to zero the command signal: $(V_{com} + V_{offs} + V_{comp}) = 0$, and then multiplying together the gains of all the considered blocks. Then

$$G_{loop}(s) = -3300 \cdot G_c \cdot \frac{R_m}{R_m + R_s} \cdot \frac{1}{1 + s\tau_d} \cdot \frac{1}{1 + s\tau_{hv}} \cdot \frac{1}{1 + s\tau_m \frac{R_s}{R_s + R_m}} \cdot \frac{s^2(\tau_+ + \tau_c) + s(\tau_c + \tau_+(1 + G)) + (1 + 2G)}{1 + s\tau_c}$$

G_{loop} has four negative real poles. Finally the response $V_m(s)$ as a function of the command (that must be inverted and scaled by 1/10) is

$$\begin{aligned} V_m(s) = & \frac{1}{1 - G_{loop}(s)} \left\{ 3300 \cdot G_c \cdot \frac{R_m}{R_m + R_s} \cdot \frac{1}{1 + s\tau_d} \frac{1}{1 + s\tau_{hv}} \cdot \right\} \\ & \left\{ \frac{2G + 1 + s\tau_c}{1 + s\tau_c} \cdot \frac{1}{1 + s\tau_m \frac{R_s}{R_s + R_m}} \right\} \cdot \left(\frac{-\frac{1}{10}(V_{com} + V_{offs} + V_{comp})(s)}{1 + s\tau_{filter}} \right) \\ & = T(s)\hat{V}(s) \end{aligned}$$

where $\hat{V} \equiv -(V_{com} + V_{offs} + V_{comp})/10$.

We see that at steady state ($s = 0$) the membrane voltage is

$$V_m(0) = \hat{V} \cdot \frac{\beta K}{1 + \beta K} \tag{4.2}$$

where $\beta \equiv R_m/(R_m + R_s)$ and $K \equiv 3300 \cdot G_c(2G + 1)$. Assuming the values in section 3.3.1 for the various parameters, β is approximately 0.4; and βK

varies in the range $[590, 5 \cdot 10^5]$, so that a good fidelity to the command signal can in principle be obtained.

The transfer function of the system $T(s)$ is a ratio of polinomials and the poles of the function are the solutions of a polinomial of 5^{th} order. As a consequence (see Korn and Korn, 1968) the membrane potential $V_m(t)$ will be a sum of five terms, each term being time–dependent through an exponential factor (in the more frequent case of poles with multiplicity one). The time coefficients in the exponents of the five exponentials are a combination of the frequencies $1/\tau_d$, $1/\tau_{hv}$, $1/\tau_c$, $1/\tau_{filter}$, $1/\tau_l$, with $\tau_l = \tau_m R_s/(R_s + R_m)$, and of the coefficients of s in the numerator of G_{loop}. The bigger time constant in the voltage clamp circuit is τ_d, (varying between 2.2 msec and 22 msec). The membrane–load relaxation time τ_l is approximately 0.28 sec (assuming for R_s and R_m the values of section 3.3.2).

If one makes a very rough approximation assigning non–zero value only to the two time constants τ_l, τ_d, then, as $\tau_l \gg \tau_d$, we have a 'fast' clamp in the sense of Katz and Schwartz (see section 3.2). The rapidity of the clamp is about $8 \cdot \tau_d$, (Katz and Schwartz, 1974) so it goes from a few milliseconds up to a few tenth of milliseconds. This corresponds in fact to the measurements (see next section).

4.3 Construction of the amplifiers

We manifactured the hardware realization VCX0 of the voltage clamp circuit in fig. 4.4 by soldering the various electronic components on normal boards and then using wires on the back side of the board to connect them (no printed boards were used).

The VCX0 contains four boards. In the first (B1) we realised the voltage preamplifier, the second (B2) contains the voltage clamp amplifier circuit (fig. 4.3) excepted the final power stage; amplifier $A5$ (block 5 in fig. 4.6) is in the third board (B3). The fourth board (B4) was used to divide by 100 the input signal to the monitor placed in the front panel. This was only done because the monitor we used accepts $\pm 199.9\ mVdc$ as input range, and

we wanted to measure up to $\pm 10V$ signals.

The circuit is contained in a metal box. The front and rear panel elements are described in fig. 4.8 and 4.9. In the front panel one finds 1) the knobs and switches for controlling the variable elements of the voltage clamp system; 2) the BNC plugs for input and output signals. In the rear panel there are the connections to the power lines ($\pm 15Vdc$ and $220Vac$) and other signals output plugs.

The metal box was bought in an electronic shop; after having designed the front and rear panel, the corresponding holes in the metal box were cut with an electrodrill.

We present, in figures 4.7–4.13, a complete description of the VCX0. Fig. 4.7 is a top view of the circuit, indicating the position of the various boards and the location of the power line. Fig. 4.8–4.13 describe the four boards. The function of all the inputs and outputs to and from the boards is given in the legends, together with the specification of the chips and other components used.

The symbols correspond to the symbols defined in the circuit schemes of figures 4.3 and 4.2.

The symbols tr1,tr2,....tr15 correspond to trimmers, i.e. variable resistances. They are used for two different functions: trimmers tr2, tr3, tr7–tr12 and tr14 serve to adjust to zero the offset voltage of the operational amplifiers P1, P2, P3 and A1–A7 respectively. The operational amplifiers have an intrinsic offset voltage which is summed to the expected output signal, due to non–ideality of their functioning. The offset compensation is made by setting the inputs of the opamps so as to expect zero output. The output is observed, and if it is non–zero, it is adjusted by changing the trimmers regulation. In the case of the voltage followers P1 and P2, for example, a zero output is expected if the positive input is set to zero. Another method for the offset voltage compensation is useful in the case of amplifier P3. P3 is in the differential amplifier configuration. If a sequence of steps is given to the positive input, and the negative input is short circuited to the positive

input, then the output should be zero, and an eventual offset voltage is easily detected. Similar procedures are used for the other amplifiers.

Trimmers tr4, tr5, tr6 and tr13, tr14 are needed for a fine regulation of the feedback resistance or the input resistance of amplifiers P3, P4, A4 and A5. The value of the feedback and input resistances is critical in determining the opamp's gain (see equation 4.1), and it must be very precisely settled especially at critical points of the circuit as those represented by P3, P4, A4 and A5.

The voltage clamp circuit VCX0 was tested on a model passive membrane simulated by the circuit of fig. 4.14. Here R_s, R_m had the values 2.21 $M\Omega$ and 1 $M\Omega$ respectively, so that β (see section 4.2) was 0.31. The VCX0 internal time constants can be varied by varying τ_d with the 'frequency response' switch (n° 9 in fig. 4.8) and also by varying the current gain G_c and the comparator gain G (potentiometer n° 11 and 10 respectively in fig. 4.8).

We tested the system's fidelity and rapidity by checking t_{95} (time for attainment of 95% of the final value) and the V_m steady state value for 50 mV–amplitude command pulses (from –25 to 25 mV) given at 100 Hz frequency (each pulse had a duration of 5 msec). The current gain G_c was maintained at a fixed value of 1 and the critical damping condition (see section 3.2) was searched by fixing τ_d and varying G up to the maximum possible value that did not produce oscillations; this was repeated for each of the four available τ_d values.

We report here the value of V_m/V_c at steady state and of t_{95} for the four possible values of τ_d. A difference between the steady state value of V_m from V_c is practically undetectable with the precision of measurement used (± 1 mV) and given the instrumentation background noise of 2 mV r.m.s. (but there was $\sim$ 1.5 mV r.m.s noise in the input signal). For τ_d=4.8 and 2.2 msec the test circuit went into oscillation for any possible gain value. Thus the two set of measurable values found are

τ_d	$G(crit)$	$V_m/V_c(steady\ state)$	t_{95}
22 $msec$	94	25	2 $msec$
11 $msec$	88	25	0.5 $msec$

where G(crit) is the value of G at critical damping. In fact, if one computes the expected steady state V_m from the formula (4.2.): $V_m = \hat{V} \cdot \frac{\beta K}{1+\beta K}$, with $\beta = 0.31$ and $K = 3300 \cdot 1 \cdot (2G + 1)$, one sees that a difference between V_m and the command value could only be seen with a precision of at least $2 \cdot 10^{-6}$ mV, which is unfeasible. The t_{95} is in the range expected.

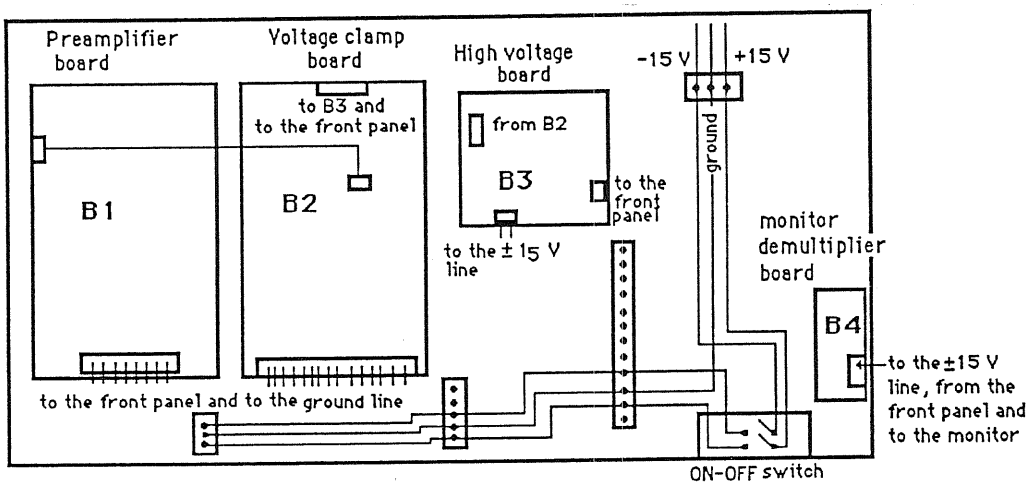

Fig. 4.7. Top view of the VCX0 boards arrangement. The power line connections and the general switch are also indicated. For each board, the starting or endpoint of wire connections is drawn together with the indication of the destination or origin of the connection.

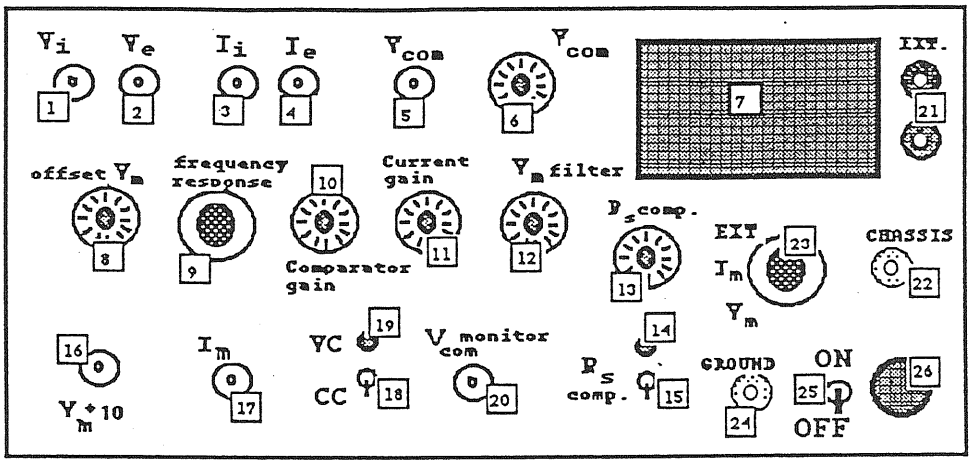

Fig. 4.8. Front panel of VCX0.

1 Internal voltage BNC input plug. Receives signal from the internal voltage microelectrode.

2 External voltage BNC input plug. Receives signal from the external voltage electrode.

3 Internal current BNC input plug. Receives signal from the internal current microelectrode.

4 External current BNC input plug. Receives signal from the external current electrode.

5 Command voltage BNC input plug.

6 Offset regulation of the command voltage: adds a variable offset value to the externally supplied V_{com}.

7 Monitor. It displays the signal selected by the switch n.23. The displayed signal is in the range $\pm$ 19.9 V, the first figure on the left being in the range 10–90 mV.

8 Offset compensation for the measured potential. Adds a variable offset value to the measured $V_i - V_e$.

9 Frequency response switch. Switches the capacitor in the feedback loop of the differential amplifier A3 between the values 10, 22, 50 and 100 nF.

10 Comparator gain. Varies the value of the gain G (see text) between 1.98 and 200.

11 Current gain. Varies the value of G_c (see text) between 0.09 and 1.

12 V_m filter. Filters the command voltage (already summed up with the offset and eventually series resistance compensation voltage).

13 R_s compensation. Varies the series resistance compensation voltage from 0 to 0.2 times $-I_m \cdot (1M\Omega)$.

14 Series resistance compensation led indicator. The led light is on when the compensation feedback loop is connected.

15 Series resistance on–off switch. The switch is on in the downward position.

16 Output voltage BNC plug. Gives $(V_i - V_e) \cdot 10$.

17 Output current BNC plug. Gives a voltage corresponding to I_m, with a fixed gain factor of 1 mV/nA.

18 Voltage clamp/Current clamp switch.

19 Voltage clamp led indicator. The led light is on when the voltage clamp option is chosen.

20 Command voltage output BNC plug. Monitors the command signal at the output of the command signal filter.

21 The red plug signal - black plug signal corresponds to the signal selected by selector n.23.

22 Connection to the chassis.

23 Selects the input signal to the monitor between the current output (n. 17) and the voltage output (n. 16). EXT position is not connected.

24 Connection to the VCX0 earth.

25 General ON/OFF switch. Connects the $\pm$ 15 V power line to the voltage clamp circuit.

26 ON/OFF switch led indicator.

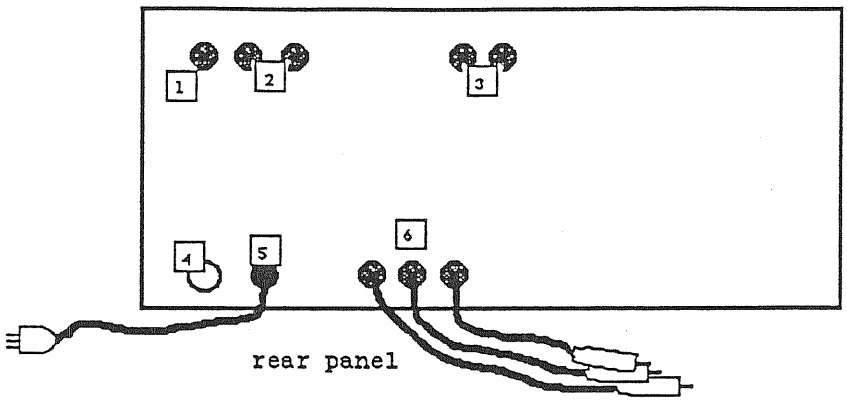

Fig. 4.9. Rear panel of VCX0.

1 Not used.
2 Red plug signal – black plug signal gives the same signal supplied to the monitor n.7 in the front panel.
3 Red plug signal – black plug signal gives the signal selected by the separator n. 23 in the front panel.
4 Switch for the input 220 Vac line alimenting the monitor.
5 220 Vac input.
6 $\pm$ 15 Vdc and earth inputs.

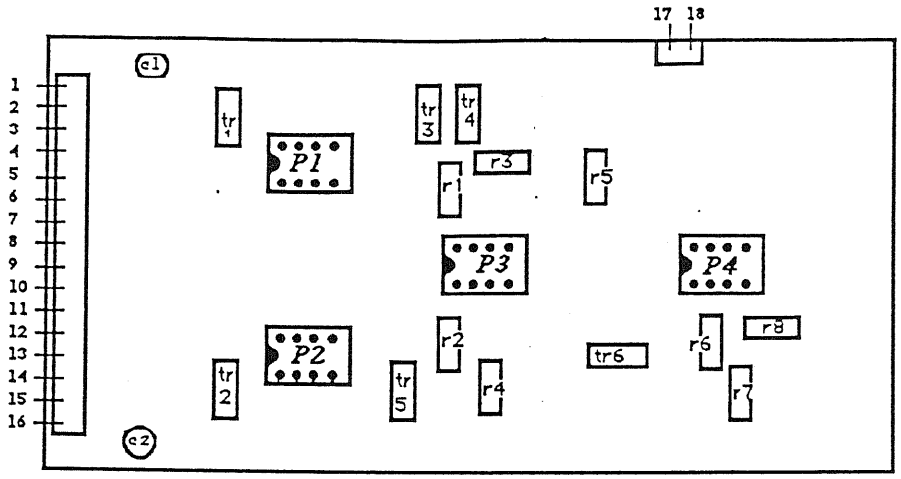

Fig. 4.10. Preamplifier board B1. P1, P2 are LF357N opamps (National Semiconductors Corporation, NSC). P3, P4 are LF356N opamps (NSC). tr1, tr2, tr3 are 10 K trimmers. tr4, tr5 are 5 K trimmers. tr6 is a 500 ohms trimmer. C1, C2 are 10 μF,85 $^{\circ}C$ capacitors. All I/O connections are indicated below (all even numbered 1–15 connections are grounded).

2	+15 V input.
4	-15 V input.
6	To offset regulation (n.8 in the front panel).
8	$V_m \cdot 10$ output to n. 16 in the front panel.
10	Grounded.
12	V_e input from n.2 in the front panel.
14	Grounded.
16	V_i input from n.1 in the front panel.
17	Grounded.
18	$V_m \cdot 10$ output to board B2.

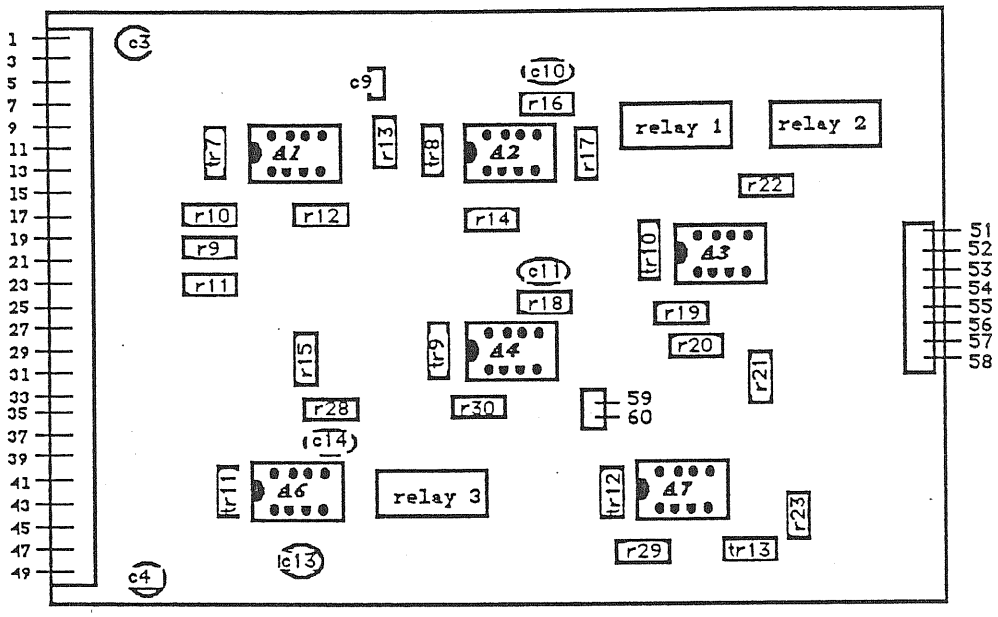

Fig. 4.11. Voltage clamp amplifier board B2. A1, A2, A4, A6 and A7 are LF356N opamps (NSC). A3 is a LF357N opamp (NSC). Relays are Hamlin–HE721C12–10 (12 V). All offset trimmers: 20 K. Feedback trimmer of A7: 5 K. Filter capacitors in the power line: 4.7 μF. Separators: 2·6–way (FEME, Italy). All I/O connections are indicated below (all even connections 2–50 are grounded).

1 + 15 V input
3 − 15 V input
5 Not used.
7 Current clamp/Voltage clamp switch
9 I_m output to n. 17 in the front panel.
11 Not used.
13 I_m input from n. 4 in the front panel.
15 Not used.
17 Not used.
19 Input from R_s switch n. 15 in the front line to relay n. 3.
21 Output to the separator n. 9 in the front panel.
23 Input from the separator n. 9 in the front panel.
25 Not used.
27 Output to R_s regulation n. 13 in the front panel from the I/V converter A6.
29 Output to G regulation n. 10 in the front panel.
31 Input from G regulation n. 10 in the front panel.
33 Not used.
35 Output to filter n. 12 in the front panel.

37 Input from filter n. 12 in the front panel.
39 Not used.
41 Input from R_s regulation n. 13 in the front panel to the summation point of A1.
43 Output to V_{com} monitor n. 20 in the front panel.
45 Input for V_{com} from n. 5 in the front panel.
47 Not used.
49 Input from offset V_{com} regulation n. 6 in the front panel.
51 I_m output to the current gain G_c regulation n. 11 in the front panel.
52 Grounded.
53 Grounded.
54 Grounded.
55 Input from the current gain G_c regulation n.11 in the front panel.
56 Current signal output from the current gain regulation to the H–V board.
57 Grounded.
58 Grounded.
59 Grounded.
60 $V_m \cdot 10$ input from board B1.

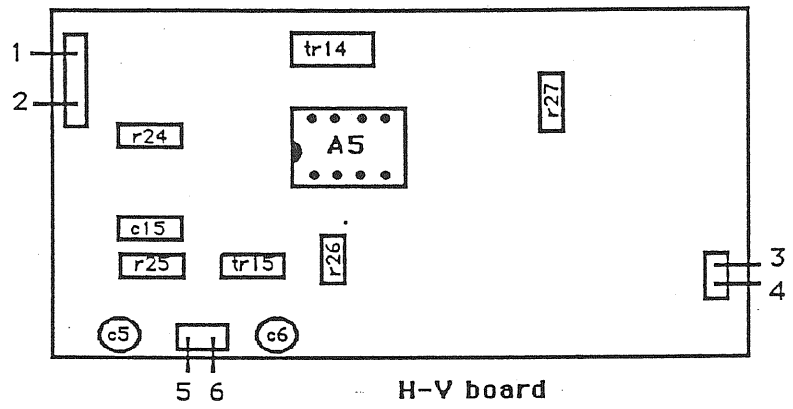

Fig. 4.12. High–voltage board B3. A5 is a $\pm 120V$ high voltage opamp (Analog Devices 171J). tr1 and tr2: 20 K c5 and c6: 4.7 μF. All I/O connections are indicated below.

1 Input I_m signal from board B2.
2 Grounded.
3 Grounded.
4 I_i output to n. 3 in the front panel.
5 +15 V input.
6 −15 V input.

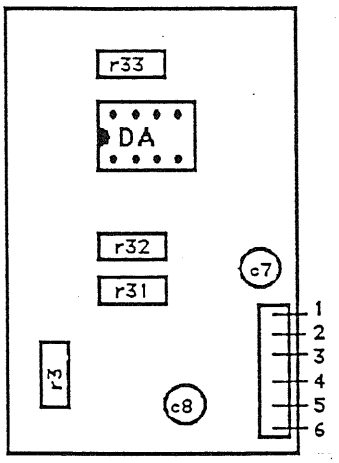

Fig. 4.13. Monitor demultiplier board. DA is an LF356N opamp (NSC). c7 and c8: 10 μF. All I/O connections are indicated below.

1 −15 V input.
2 Input to the non-inverting input of DA.
3 Output signal to the monitor.
4 Input to the inverting input of DA.
5 +15 V input.
6 Grounded.

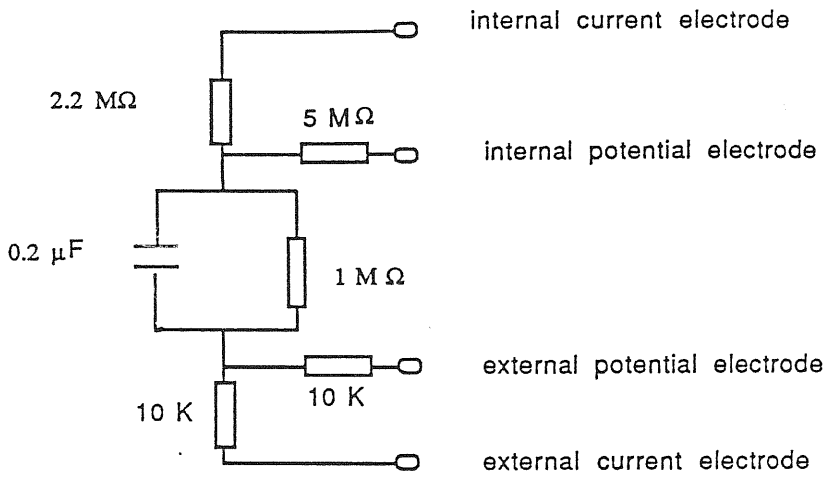

Fig. 4.14: Simulation of a model passive oocyte membrane connected to microelectrodes.

Chapter 5

Methods for voltage clamp experiments on Xenopus oocytes

We shall describe here with some detail the procedures used in our experiments for obtaining oocytes from the frog *Xenopus laevis*, for the preparation of the oocytes to voltage clamp experiments, and for the voltage clamp experiment itself.

5.1 *Xenopus* maintaining.

Twenty *Xenopus laevis* females were kept in a fish tank of $30 \cdot 80 \cdot 50$ cm in $\sim 8 - 10$ cm of water, with a continous water flow. Normally it is possible to use tap water. However, when the water contains an excessive amount of chlorine, it is advised to eliminate it, by exposing the water to air for a long time before its use, or by de–ionizing it. The walls of the tank were covered with opaque–dark paper, so as to avoid disturbing the frogs with unfamiliar pictures, because we noted that they were otherwise very excited. The animals were fed once a week with diced liver ($\sim 50g$ for 20 frogs).

5.2 Oocytes extraction and storage.

For the study of expression of foreign membrane proteins immature oocytes are needed. To obtain immature oocytes one has to extract the oocytes from the mother frog's ovary. Immature oocytes are germ line cells that have entered meiosis and are arrested in the first prophase stage. During this first prophase stage they develop very slowly, passing through six morphologically characterized stages (Dumont, 1972; Dumont and Brumett, 1978); in their membrane the native density of ionic channels is very low. In

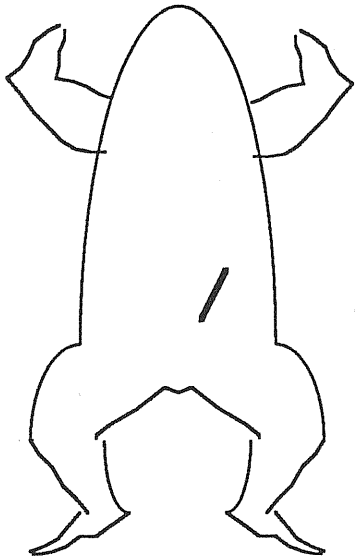

Fig. 5.1: Abdominal cut for oocytes extraction from an anesthetized frog.

the most developed stages, V and VI, the oocytes are ~ 1.2 mm in diameter, and their surface is divided into two hemispheres: a dark brown ('animal') and a yellow ('vegetal') hemisphere. Oocytes in the process of maturation show white speckles in the animal pole or dark speckles in the vegetal pole. They must be avoided for the expression experiments.

For the extraction the frogs were anesthetized by keeping them for $\sim 10-15$ minutes in water and ice. Usually frogs anesthetized faster if their head was immersed in minced ice. A small abdominal cut ($\sim$ 1 cm) was made in the frog skin and abdominal muscle to one side of the midline, ~ 1 cm above the bladder (see fig. 5.1). A part of the ovary was exposed by pressing lightly the abdomen around the cut, and a piece of it was dissected. The frog was sutured with sterile silk and put in water at room temperature, where it recovered almost immediately. After a few hours it was returned to the tank.

The extracted part of the ovary consisted of a few ovarian lobes: they are small sacs of epithelial cells ruptured at some ends, containing the follicles, i.e. oocytes plus follicular cells. The lobes were moved with forceps to Petri dishes containing modified Barth's solution with antibiotics (see section 5.4), and stored at 18°C. Oocytes stored inside the lobes remained viable for some days (sometimes more than 10 days), while oocytes stored after separation from the ovarian wall (see next section) were more fragile and broke after 4–5 days.

Chapter 5

Methods for voltage clamp experiments on Xenopus oocytes

We shall describe here with some detail the procedures used in our experiments for obtaining oocytes from the frog *Xenopus laevis*, for the preparation of the oocytes to voltage clamp experiments, and for the voltage clamp experiment itself.

5.1 *Xenopus* maintaining.

Twenty *Xenopus laevis* females were kept in a fish tank of $30 \cdot 80 \cdot 50$ cm in $\sim 8 - 10$ cm of water, with a continous water flow. Normally it is possible to use tap water. However, when the water contains an excessive amount of chlorine, it is advised to eliminate it, by exposing the water to air for a long time before its use, or by de–ionizing it. The walls of the tank were covered with opaque–dark paper, so as to avoid disturbing the frogs with unfamiliar pictures, because we noted that they were otherwise very excited. The animals were fed once a week with diced liver ($\sim 50g$ for 20 frogs).

5.2 Oocytes extraction and storage.

For the study of expression of foreign membrane proteins immature oocytes are needed. To obtain immature oocytes one has to extract the oocytes from the mother frog's ovary. Immature oocytes are germ line cells that have entered meiosis and are arrested in the first prophase stage. During this first prophase stage they develop very slowly, passing through six morphologically characterized stages (Dumont, 1972; Dumont and Brumett, 1978); in their membrane the native density of ionic channels is very low. In

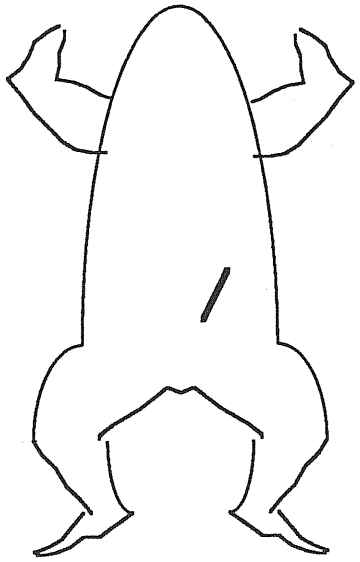

Fig. 5.1: Abdominal cut for oocytes extraction from an anesthetized frog.

the most developed stages, V and VI, the oocytes are ~ 1.2 mm in diameter, and their surface is divided into two hemispheres: a dark brown ('animal') and a yellow ('vegetal') hemisphere. Oocytes in the process of maturation show white speckles in the animal pole or dark speckles in the vegetal pole. They must be avoided for the expression experiments.

For the extraction the frogs were anesthetized by keeping them for $\sim 10-15$ minutes in water and ice. Usually frogs anesthetized faster if their head was immersed in minced ice. A small abdominal cut ($\sim$ 1 cm) was made in the frog skin and abdominal muscle to one side of the midline, ~ 1 cm above the bladder (see fig. 5.1). A part of the ovary was exposed by pressing lightly the abdomen around the cut, and a piece of it was dissected. The frog was sutured with sterile silk and put in water at room temperature, where it recovered almost immediately. After a few hours it was returned to the tank.

The extracted part of the ovary consisted of a few ovarian lobes: they are small sacs of epithelial cells ruptured at some ends, containing the follicles, i.e. oocytes plus follicular cells. The lobes were moved with forceps to Petri dishes containing modified Barth's solution with antibiotics (see section 5.4), and stored at 18°C. Oocytes stored inside the lobes remained viable for some days (sometimes more than 10 days), while oocytes stored after separation from the ovarian wall (see next section) were more fragile and broke after 4–5 days.

5.3 Oocytes preparation for voltage clamp experiments.

Voltage clamp experiments were made both on follicles and on defolliculated oocytes at stages V and VI . Follicles are oocytes surrounded by their complete 'envelope' as it appears in the intact ovary. The envelope consists of several layers with different structures: in contact with the plasma membrane of the oocyte there is the vitelline membrane, a thin non–cellular layer. It is covered externally by the follicular cells, a monolayer of small cells, much smaller than the oocyte. It follows the theca, a non–cellular fibrous layer, with unevenly distributed fibroblasts. Finally, a monolayer of epithelial cells makes the connection between the oocyte and the wall of the ovary (see fig. 5.2).

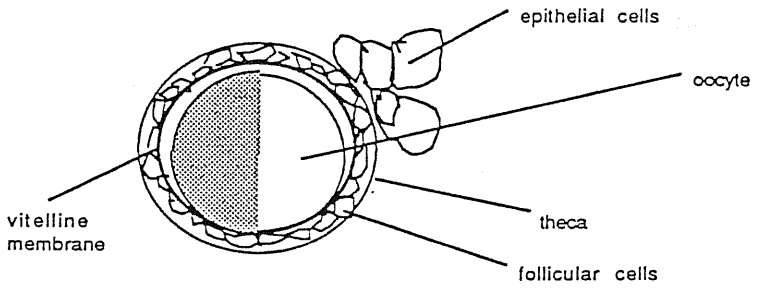

Fig. 5.2. Schematic representation of an oocyte surrounded by its 'envelope'. The dimensions of the vitelline membrane and follicular cells relative to the oocyte are slightly magnified.

Isolated follicles were obtained by cutting with iridectomy scissors the epithelial cells connecting them to the ovary. After isolation the single follicles were handled with a wide–tipped Pasteur pipette whose tip was broken and smoothed with a flame.

For experiments on defolliculated oocytes, the follicles were treated enzymatically and mechanically to obtain the denuded oocytes. Each follicle was placed for $\sim$ 1 hour in modified Barth's solution with collagenase (1 mg/ml). The type of collagenase and the duration of the immersion is a critical parameter determining the viability of the oocyte membrane: we used two different batches of collagenase (Sygma, type VII and Sigma, cell culture–tested) which probably were both unfit for the purpose, because the membranes were subsequently very delicate (see section 6.1). In fact, it is

proposed in the literature to use collagenase Sygma type I (e.g. in Barish, 1982; Dascal et al., 1984; Methfessel et al., 1986) or Sigma type II (Barnard and Bilbe, 1987).

After the collagenase treatment, the follicles were removed by means of fine forceps and stored in modified Barth's solution plus antibiotics for later experiments. We add here that, for patch–clamp experiments on the oocyte, the removal of the vitelline membrane is also necessary to free the access to the oocyte membrane. This is a more delicate procedure; we tried it, but the patch–clamp experiments were not possible because of many problems, which we enumerate in section 6.1, the main problem being possibly that, as is reported by other researchers, the membranes are very fragile in summer, and our attempts were carried on in summer. To remove the vitelline membrane, the defolliculated oocyte must be placed (at least some hours after the collagenase treatment, or the day after) in an hyperosmotic solution ('stripping' solution, see section 5.4) for a few minutes. The oocyte slowly shrinks because of the osmotic gradient, and the vitelline membrane becomes separated from the oocyte, so that it can be mechanically removed by appropriated forceps. During this manipulation very frequently the oocytes are damaged or broken.

After the removal the oocyte is very fragile, and it should not be exposed to the water–air interface, at risk of serious damage; it is washed in Ringer solution (see section 5.4) and placed in the middle of a Ringer–containing Petri dish, where it adheres spontaneously to the bottom of the dish. In about half an hour the oocyte is ready for patch clamp.

The techniques exposed in this section are, apart from minor variations, the general used techniques for defolliculation and for vitelline membrane removal (see Barnard and Bilbe, 1987; Methfessel et al., 1986). Some researchers (Methfessel, 1986; Taglietti and Toselli, 1988) have used also a protease treatment to remove the vitelline membrane, which should be however (Methfessel et al., 1986) less effective for a complete removal.

5.4 Solutions.

The compositions of all the solutions used are reported in table 5.4.1 and 5.4.2. The Ringer solution simulates the normal physiological extracellular medium and was used during all voltage clamp tests as control medium. The modified Barth's solution is similar to Ringer, but with a lower osmo-

Solution	$NaCl$	KCl	$CaCl_2$	$CaNO_3$	$NaHCO_3$	$MgSO_4$	$TrisHCl$	$Hepes$	$Osmolarity$
Ringer	115	2.5	1.8	–	–	–	–	10	250.4
Barth's	88	1	0.41	0.33	2.4	0.82	7.5	–	201.3
'Sodium'	117.5	–	1.8	–	–	–	–	10	250.4
'Potassium'	–	117.5	1.8	–	–	–	–	10	250.4

Table 5.4.1. Solutions for voltage clamp experiments. Barth's solution, pH=7.6. Other solutions, pH=7.4. All concentrations in mM, osmolarity in mOsm..

Solution	KCl	$MgCl_2$	$K^+asp.$	$K^+gluconate$	$EGTA$	$EDTA$	$Hepes$	$Osmolarity$
Stripping 1	20	1	200	–	10	–	10	475
Stripping 2	20	–	–	262	–	10	10	600

Table 5.4.2. Hyperosmotic solutions (pH=7.4) for vitelline membrane removal. All concentrations in mM. Osmolarity in mOsm..

larity, and was used for oocytes storage. The solutions where the K^+ and Na^+ concentrations are varied were used for experiments on the K^+ dependence of the membrane resting potential in the assumption that Na^+ changes had little effects (but see section 6.2 for a discussion on the validity of this assumption). The variable K^+ and Na^+ concentrations were obtained by mixing in different proportions the reported 'sodium' solution and 'potassium' solution. In a few tests acetylcholine (Sigma) $10^{-5}M$ was added to normal Ringer solution. In modified Barth's solution the pH was 7.6. All other solutions had a pH of 7.4. Penicillin 100 U/ml and streptomycin 100 mcg/ml (Gibco) were added to modified Barth's solution for oocyte storage.

5.5 Microelectrodes.

To make a double electrode voltage clamp two pairs of electrodes are needed, each pair being consituted by an intracellular electrode and a bath electrode. The first pair is used for voltage recording, the second one for current injection. In the first case, the bath electrode gives the reference

voltage relative to which the membrane voltage is measured. In the latter case, current is injected by the intracellular electrode and it is recorded by the extracellular bath electrode, which makes a virtual–ground connection to earth.

We used the arrangement shown schematically in figure 5.3 for the connection of the four electrodes. All the electrodes were $Ag/AgCl$ reversible electrodes. The internal electrodes were made with glass pipettes with very small tip (in the micrometers range, see below) on one end. The pipettes were filled with a 3 M KCl salt solution in the case of the voltage recording internal electrode, and with 500 mM K_2SO_4, 30 mM KCl in the case of the internal current electrode respectively. The other end of the pipettes were in contact with a clorurated silver wire making the connection with the voltage clamp circuit. The two external electrodes were made by agar–bridges. The external voltage electrode–bridge was made with 0.5 % (in weight) agar powder in 3M KCl solution. The mixture must be made at $\sim 60/70°C$: it appears as a liquid when hot, and it turns to a jelly at room temperature. The jelly (i.e. the bridge) was injected while it was still hot in small plastic tubings. The tubings connected the bath with a 3 M KCl solution. This latter was in turn in contact with an $Ag/AgCl$ electrode made with a clorurated silver wire. An analogous procedure was used to make the external current–agar bridge, with the substitution of the 3M KCl solution with a 500 mM K_2SO_4, 30 mM KCl solution. With the above scheme there was symmetry in the wire–solution connections so that in each pair of electrodes the equilibrium potential for the exchanged ion (chloride) at the wire–solution interface was equal in the external and internal electrode. In such a way the two equilibrium potentials canceled out in the measurements. If the bath electrode had consisted only in a chlorurated silver wire immersed in the bath, an offset potential would have been present because of the different chloride concentration in the solutions surrounding the wires.

The glass pipettes for intracellular voltage recording and current injection were both made with borosilicate glass capillaries (Hilgenberg), and pulled with a two–stage procedure by a patch–clamp puller (L/M–3P–A, List). Care was taken to obtain pipettes with as long as possible shanks, compatible with the tip width required. This was done because during the electrode insertion the oocyte membrane used to distort while resisting to penetration, and then suddenly it ruptured and resealed around the pipette, with a long portion of the pipette enclosed in the oocyte. A short shank, with its associated large diameter at short distances from the pipette tip, resulted

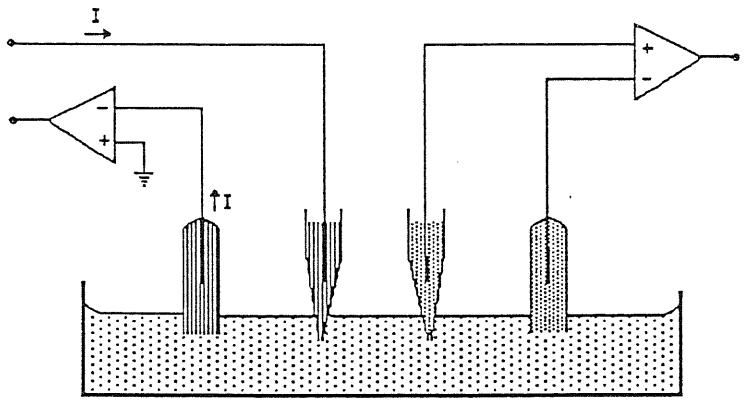

Fig. 5.3: The arrangement of the two pairs of electrodes of a double–microelectrode voltage clamp. Each pair consists in two $Ag/AgCl$ electrodes inserted in a micropipette and in an Agar bridge respectively, in contact with a concentrated salt solution.

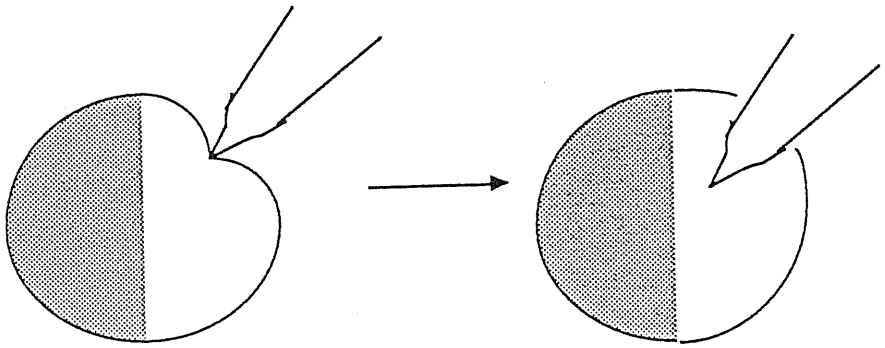

Fig. 5.4: The insertion of a micropipette in an oocyte membrane. After insertion a long portion of the pipette beyond the tip remains inside the oocyte.

in a big hole in the oocyte membrane and in oocyte damage (see fig 5.4). The voltage and current pipettes were made in the same way; their resistance was $\sim 1.5M\Omega$. The resistance was measured by the method schematically shown in fig. 5.5.

Offset signals recorded from the bath could usually be attributed to asymmetry in the cloruration of the internal and external voltage and respectively current electrodes (the asymmetry consists in a relative depletion of disposable chloride ions at the wire–solution interface, resulting in a different chloride equilibrium potential). The differences in cloruration could

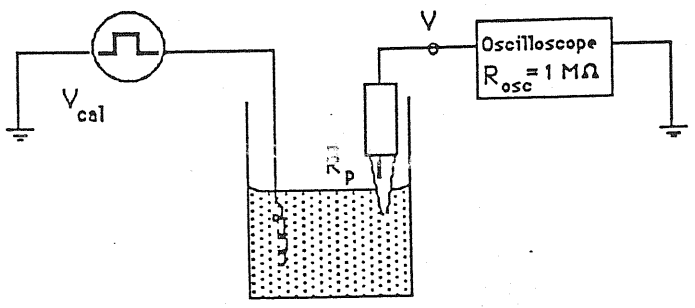

Fig. 5.5: Arrangement for measurement of microelectrodes resistance. A BNC plug was completed with a holder and a clorurated silver wire at one end, and connected to an oscilloscope (Tektronix, 5111A storage oscilloscope, with $1M\Omega$ input resistance) at its other end. The pipette filled with the concentrated salt solution – either 3 M KCl or the current electrode solution (see text) – was mounted on the holder and then immersed in Ringer; a calibration signal (provided by the same oscilloscope) was applied to the solution with a normal wire (whose resistance was approximated to zero in our calculations). The signal received by the oscilloscope, V, was measured and was related to the microelectrode resistance R_p by the voltage–divider formula: $V{=}V_{cal}{\cdot}((R_{osc}/(R_{osc}{+}R_p))$, so that $R_p{=}R_{osc}{\cdot}(\frac{V}{V_{cal}}{-}1)$.

be eliminated by leaving the electrodes in the bath overnight, better if facilitating the chloride movement between the electrodes by breaking the tip of the glass pipettes (a slow reequilibration occured spontaneously). The usual value of any offset potential in our measurements was between 0 and ±10 mV, so that it could be easily compensated, and remained relatively constant during the measurements.

The oocyte membrane is not eccessively damaged by the insertion of glass pipettes with tip resistance of $\sim 700K\Omega - 1M\Omega$ (see Dascal et al., 1984, for a study on the recovery of membrane potential after the insertion of microelectrodes). These resistances correspond, in the recording conditions used with oocytes, approximately to $\sim$ 0.5 μm tip diameter (see Purves, 1981) A $1M\Omega$ resistance is a very low value of resistance if compared to the resistances needed for recording from viable smooth muscles (25–50 $M\Omega$, Purves 1981). A low resistance is a very favorable condition for a reliable voltage recording and current injection.

In fact, a high microelectrode resistance has negative effects on a number of factors determining the performance of a voltage clamp circuit: tip potential, current passing ability and consequently clamping fidelity, noise and interference pick–up, and circuit time–constant (Purves, 1981). A mi-

croelectrode with a small tip and a big resistance, moreover, can easily show a non–linear, time dependent I–V characteristic, i.e. a variable resistance, where the non linearity is evident for consistent values of the current, of the order of tenths of nanoamperes or less, so that it is impossible to use them reliably for any measurement. In the case of oocytes, as a consequence of the low microelectrode resistance, precautions as the 'negative–capacitance' compensation feedback to avoid filtering of the input voltage signal are not needed.

The choice of KCl as the electrodes filling solution comes from the fact that K^+ and Cl^- have similar diffusion coefficients and carry unit charge. Therefore only a small charge separation is associated with diffusion of KCl from the electrodes, and the liquid junction potential is minimized. The fairly high concentration of the filling solutions is used with the aim to obtain a high ionic concentration in the tip of the microelectrodes, and consequently a low resistance.

5.6 The voltage clamp set–up.

The set–up for voltage clamp consisted in

– an inverted microscope (CK2, Olympus) on which a Petri–dish–holder was mounted.

– Two micromanipulators Mitutoyo, with coarse (0–25 mm range) and fine (0–0.002 mm) regulation of movement in three orthogonal fixed directions, one of the directions being along the vertical and the others in the horizontal plane. No movement in the direction at 45° to the vertical was possible. These micromanipulators are endowed with a magnet to fix them to any ferromagnetic horizontal base.

– Two plastic holders, mounted on the micromanipulators by means of a hand–made plexiglas connection. Some instability (but not a fatal one) derived from this connection to the set–up performances.

– A gravity bath perfusion system with two alternative flows and a sucking pump. Two plastic syringes were hung on a metallic support laying on the table, and connected through a plastic three–ways valve to small polyethylene tubings $\sim$ 2 mm in internal diameter. The two tubings converged to an Y crossroad–point and the emerging tubing could be immersed in the Petri dish. The rapidity of the solution flow depended on the adjustable height of

the syringes relative to the Petri dish, and was usually adjusted so as to have a solution flow of 2 ml/min. The sucking system consisted in a plastic tube plugging in the dish, and connected to a standard laboratory water vacuum pump, operated by compressed air. It is essential that the tube extremity plugging in the liquid is small, $\sim$ 1 mm in diameter, so as to avoid mechanical waves in the liquid and corresponding noise in the recordings.

All the above equipment was placed on a normal table. For the elimination of at least a part of the mechanical vibrations, a marble plate of $\sim$ 2 cm thickness, an aluminium plate of $\sim$ 1 cm and finally a thin iron plate, all of about the table plane dimensions, were put one over the other on the table, and fixed to it. However this attempt to reduce vibrations was quite insufficient, and a specialised anti–vibration table, or a thicker marble plate sustained by small tyres should be provided in the future. The thin iron plate by the way provided a ferromagnetic basement for the fixing of the micromanipulators to the table.

The table and the equipment on it was contained in a Faraday cage. The cage skeleton was built with wood. A thin metallic grid was mounted on the wood supports and connected to the amplifier's ground. Outside the cage, the electronic equipment was composed by

– the voltage clamp amplifier VCX0 described in chapter 4;

– a voltage gate system (LM/GPP–3, List) used for stimulation;

– a function generator (Circuitmate, FG2) used in connection with the voltage gate, for high frequency ($\geq$ 1 Hz) stimulation.

The VCX0 was powered by a $\pm 15V$ voltage supply. All the connections between the voltage clamp amplifier and the clamp electrodes were made by shielded cables with BNC plugs on one end, and gold covered miniconnectors connected to the electrodes on the other end.

5.7 Membrane voltage measurement. The oocyte membrane potential was simply measured without the need to voltage–clamp the membrane, just inserting the voltage–recording electrode in the oocyte. For this purpose the VCX0 could be switched to the 'CC' (current clamp) configuration (see fig. 4.1.2), where the voltage preamplifier was disconnected from the rest of the circuit, and used as a voltage monitor. For the experiment, a single oocyte (or follicle) was placed in the middle of a Petri dish and focused in

the microscope; the 3M KCl containing pipette was immersed in the bath; the bath offset potential was compensated, if present, by moving the 'offset V_m' knob in the VCX0; the pipette was then approached from the right to the upper part of the oocyte and inserted in the membrane. The insertion was monitored by the change in the potential value appearing in the voltage monitor in the front panel of VCX0. The problem of oocyte movement in the dish was skipped by approaching the membrane from its top and moving the pipette in the vertical direction. However we were looking at the oocyte through an inverted microscope, and it was impossible to see the pipette at the very moment of insertion. Therefore we can not be sure that this insertion procedure was not contributing to the membrane damage that we hypothesize (see section 6.1) as an explanation of the very low input resistance value obtained in almost every experiment.

After the electrode insertion, if no voltage clamp was attempted, the membrane potential was observed in the pen–recorder trace.

5.8 Voltage–clamping.

For voltage clamp, after the insertion of the voltage electrode (see last section) the current pipette was approached to the left side of the oocyte and inserted in the membrane while the voltage clamp amplifier was switched to the 'CC' configuration. After the insertion, the amplifier was switched to the voltage clamp ('VC') configuration, taking care to previously adjust the command voltage to the desired value. In our experiments the acquired data consisted essentially in the current responses to sequences of voltage pulses. The sequences consisted in pulses of 15 seconds duration given every 40 seconds, so that for 25 seconds between pulses the membrane potential was kept at the holding potential. The amplitude of the pulses increased gradually by 10 mV in the negative or in the positive direction relative to the holding potential. In such a way I–V plots were later obtained. The pulses were triggered manually using the voltage gate.

5.9 Data acquisition.

The current and voltage signals, I_m and V_m, were sent from the VCX0 to a two channel oscilloscope (a Tektronix dual–storage oscilloscope) for viewing during the experiments and, in parallel, they were sent to a PCM converter (Digital Audio Processor, PCM–50ES, Sony, Japan) and recorded on a tape–recorder (Super β Stereo Video Cassette Recorder, Sony). A third pos-

sibility was to send in parallel the signals to a two–channel pen recorder, when observing slow responses in the order of tenth of seconds or minutes. The recorded signals were retrieved from the tape–recorder/PCM system, and acquired by an ATARI 1040 ST microcomputer through a 12–bit AD/DA interface (M2–Lab,Instrutech). The AD/DA converter admitted input was ± 10 V, so that the precision of the measurements was ± 2.45 mV. The acquisition program was a KHF–BASIC program developed in our laboratory, with maximum sampling rate of 16.3 samples per second.

This sampling rate was sufficient for observing our response currents, which developed on the time scale of seconds.

The digitized data were later transferred to a PC microcomputer and elaborated using LOTUS 1–2–3.

Chapter 6

Measurement of the oocyte membrane's electrical characteristics

Essentially two kinds of test parameters were measured in our experiments, i.e. the membrane resting potential and the membrane input resistance, with the aim to test the viability of our oocytes, as well as the functionality of the voltage clamp amplifier and of the set–up.

6.1 Resting potential and membrane input resistance measurements.

The membrane resting potential V_m of many *Xenopus* oocytes from different donors was measured with a voltage – recording microelectrode (see section 5.7).

The membrane resistance was measured in voltage clamped (see section 5.8) oocytes by the following procedure, which by the way enabled also a second V_m measurement: the oocyte was clamped at a given holding potential, usually chosen first as the zero current potential and successively along the experiment changed to more negative potentials. Then depolarizing and hyperpolarizing voltage steps of 10 or 15 seconds (see figure 6.1) were applied to the clamped membrane.

An I–V curve was later plotted by selecting I as the steady state value of the current response to V. If a current was not a 'passive' one, it was discarded from the acquired data. From the I–V curve the resting membrane potential V_m was checked (V_m is by definition the zero–current potential), and the membrane resistance was computed as the slope resistance (see section 2.1) at V_m.

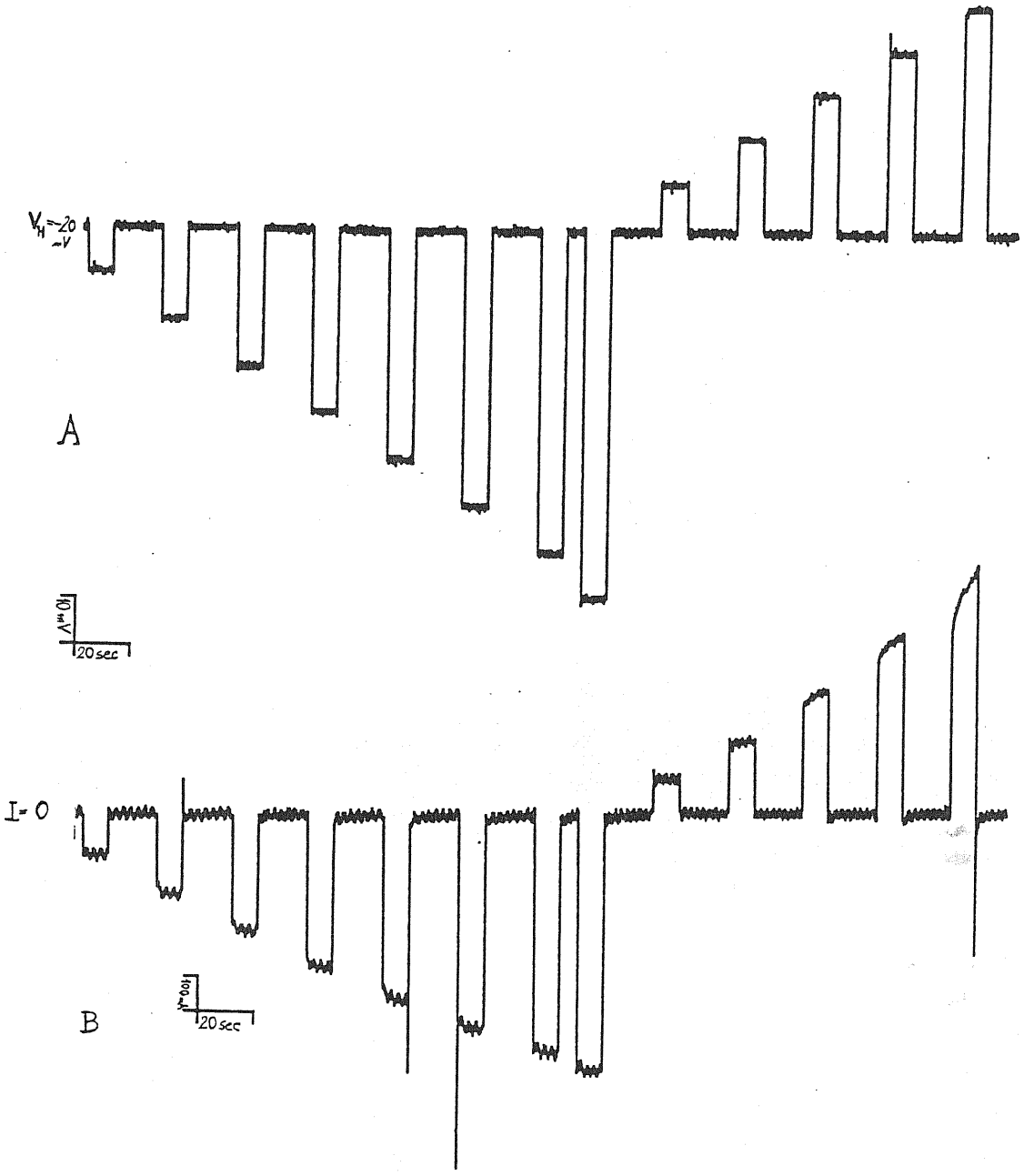

Fig. 6.1: Current response to a sequence of voltage pulses. A: Membrane potential, following a command sequence of pulses from the holding $V_h = -20$ mV. B: The membrane current I_m corresponding to the voltage sequence in A. The response is passive for $\pm$ 10 mV around V_h. Here $V_m = V_h$.

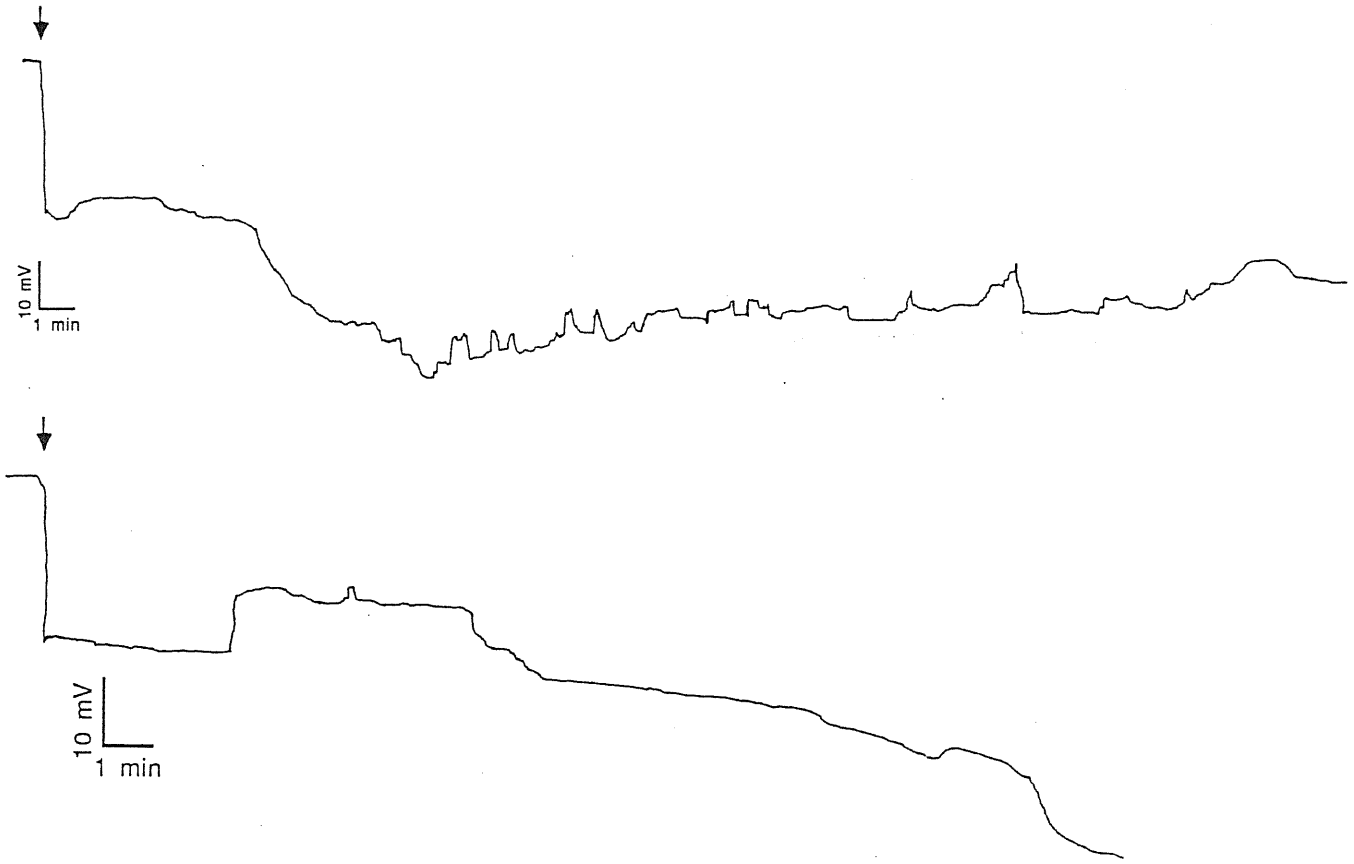

Fig. 6.2: Membrane potential oscillations in two different oocytes bathed in Ringer solution. Microelectrode insertion is marked by the arrows.

A response was considered to be 'passive' if it consisted in a capacitative peak followed by a relaxation to a steady–state value. Usually the responses were 'passive' for voltage steps of $\pm 10/20\ mV$ around the holding potential V_h. We observed various voltage and time–dependent ionic currents developing for voltage steps of greater amplitudes, but accurate studies of these currents were not yet undertaken. For a review the many voltage–dependent and transmitter–operated currents found in oocytes, see Barnard and Bilbe, 1987; Miledi, 1988.

The reason for checking V_m after stepping to each different holding potential in each oocyte was that V_m was often observed to oscillate between quite different values (see fig. 6.2). The possible origin of these variations is discussed later.

V_m was practically determined as the V–axis intercept of the straight line through the two points of the I–V curve nearest to the V–axis intercept.

The slope of the same straight line was equated to $G_m \equiv 1/R_m$. The value of R_m generally varied, in an oocyte, after changing the holding potential. All oocytes were studied from 0 to 4 days after extraction.

6.1.1 Resting potential. The average value of the resting membrane potential V_m for Ringer–bathed oocytes was $-44.5 \pm 14\ mV$ (mean $\pm$ standard deviation), as averaged over 22 oocytes from different donors, 9 of which were later voltage– clamped to measure R_m.

The values used for the average were the more stable values reached by V_m at least 10 minutes after insertion of the voltage electrode; but often a stable value was reached after 20 or 30 minutes (fig. 6.3).

This variable delay is probably connected to the different extent of the damage produced in the membrane by the insertion of the micropipette and to the difficulty for the cell to reseal the membrane, as will be discussed later (see section 6.2).

The value of V_m was not only dependent upon time after electrode insertion, but it was also very sensible to the perfusion flow of bathing solution. When the perfusion flow was stopped, V_m tended to hyperpolarize, sometimes even by 10 or 20 mV; if the flow was switched on again, V_m promptly returned near to the original value (see fig. 6.4). Most of the measurements included in the above V_m average were collected during perfusion of the oocytes.

6.1.2 *Membrane resistance.* In a set of nine oocytes from two different donors, the membrane resistance R_m, or input resistance, was computed as the slope resistance at V_m. R_m was variable, in the range $40 - 133K\Omega$, differing between oocytes and depending on the holding potential; the average resistance obtained pooling together all the measurements made at any holding potential was $72K\Omega \pm 21.3K\Omega$ (mean $\pm$ standard deviation). In table 6.1 average values are reported for R_m at various holding potentials. They show an appearent increase as V_h becomes more negative, ranging from $\approx 50K\Omega$ at $V_h = -30\ mV$ up to $109K\Omega$ at $V_h = -110\ mV$. No attempt was made to explain this increase in R_m, because of the low reliability of the all data.

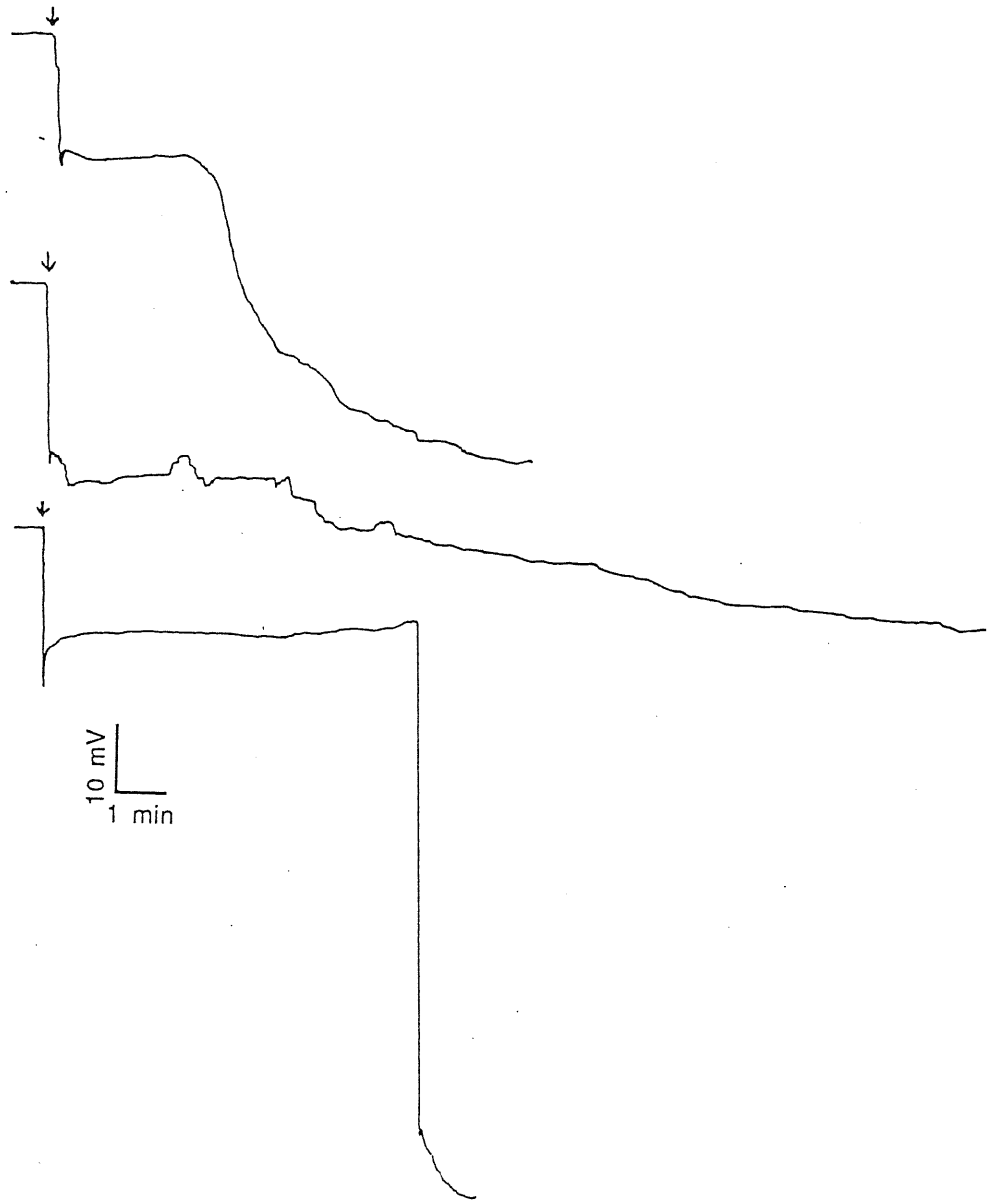

Fig. 6.3: Three examples of membrane potential repolarization after microelectrode insertion (marked by arrows). The repolarization can occur either with a very steep variation, or following a slow noisy pattern.

In fact, the average R_m value was $72K\Omega$. This is a very low value for R_m, more or less one order of magnitude lower than the average value of $714K\Omega$ reported, for example, by Kusano, Miledi and Stinnakre (1982) for oocytes at stages IV and V (Dumont, 1972), and also one order of magnitude less than the average value of $600K\Omega$ reported by Dascal, Landau and Lass

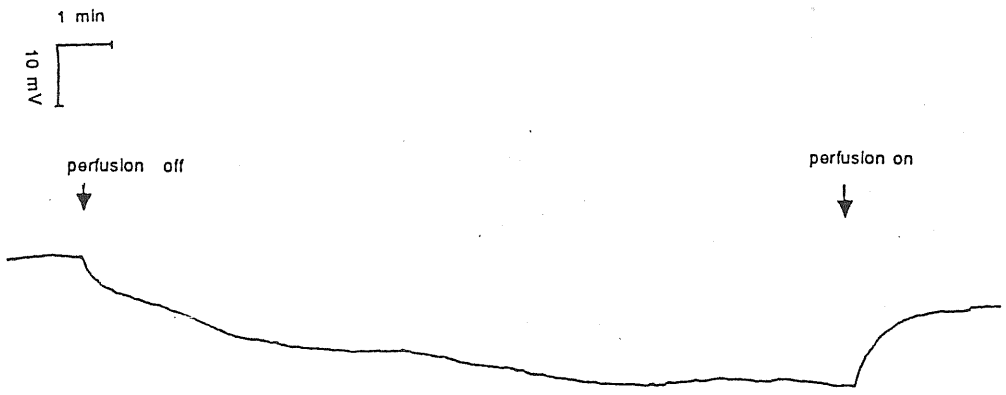

Fig. 6.4: The effect of switching off and on the bath perfusion system on the membrane potential.

V_h (mV)	R_m $(K\Omega)$	
-30	49.7 ± 27.6	$(n = 7)$
-40	69.3 ± 15.8	$(n = 3)$
-50	68.5 ± 19.5	$(n = 2)$
-60	62 ± 8	$(n = 2)$
-80	67.3 ± 5.4	$(n = 3)$
-90	102	$(n = 1)$
-110	109 ± 23	$(n = 2)$

Table 6.1. Average values of R_m (slope resistance at the membrane zero-current potential) at different holding potentials V_h (mean $\pm$ standard deviation).

(1984) for oocytes at stages V and VI. This discrepancy, probably due to an excessive damage to the oocyte membrane during the electrode insertion, will be discussed later (see next section).

The oocytes diameter (assuming a spherical shape) was measured. It resulted to be 1.22 ± 0.03 mm (mean $\pm$ standard deviation), so that the average oocyte surface was $4\pi r^2 = 0.18$ cm^2, if one neglects the presence of microvilli (see section 3.3).

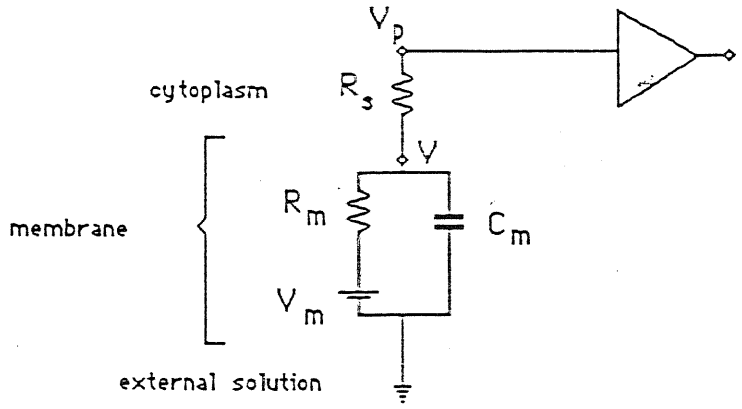

Fig. 6.5: Equivalent circuit for membrane voltage measurement.

6.1.3 *Problems in membrane capacity measurements.* We recall that the membrane capacity measurement through voltage clamp experiments proceeds as follows: a voltage step is imposed to the membrane potential, and the corresponding current change is related to the equation

$$I(t) = C_m \frac{dV(t)}{dt} + \frac{V - V_m}{R_m} \quad , \tag{6.1.1}$$

where V is the voltage sensed across the membrane, and V_m is the resting potential (see fig. 6.5). The clamped voltage is the voltage V_p at the input of the preamplifier, and differs from V by an additive factor $I(t) \cdot R_s$, where R_s is a resistance in series with the membrane, representing the voltage microelectrode resistance, and should be high compared to R_m, $R \gg R_m$. Then

$$I(t) = C_m \frac{d(V_p - I(t)R_s)}{dt} + \frac{V_p - V_m}{R_m} - I(t)\frac{R_s}{R_m} \quad , \tag{6.1.2}$$

and setting

$$\frac{dV_p}{dt} = 0 \quad , \tag{6.1.3}$$

$$\frac{dI(t)}{dt} = \frac{V_p - V_m}{R\tau_m} - I(t)\left[\frac{1}{\tau_m} + \frac{1}{R_s C_m}\right] \quad . \tag{6.1.4}$$

The solution of this equation is an exponential relaxation from an initial peak value to a steady state value, with time constant $\tau_m \cdot R_s/(R_s + R_m) \sim \tau_m$. But this is only true if we can assume the condition 6.1.3, implying that the change of the clamped potential V_p is much more rapid than the process of charging the membrane capacitance C_m.

In our experiments the measurement of the membrane capacity C_m was prohibited by the low value of the membrane resistance ($72 \pm 21.3 K\Omega$), and consequently the high value of the clamp rise time. To explain this fact, we need to keep in mind the computations of sections 3.2 and 4.2. If we simplify the description of our voltage clamp amplifier by only one instrumental time constant (see section 4.1), the voltage clamp rise time (τ_{90}) is dependent (see section 3.2) upon the membrane–solution time constant (τ_l) and the instrumental time constant (τ_d). We can guess the value of (τ_l) for the oocytes on which our experiments were made: if we assume $C_m \approx 1\mu F/cm^2 \cdot 0.18\ cm^2 = 0.18\mu F$, then $\tau_m \equiv R_m C_m = 1.26\ msec$, and $\tau_s \equiv R_s C_m = 270\ msec$, (with $R_s = 1.5 M\Omega$ the current electrode resistance), so that $\tau_l \equiv \tau_s \tau_m / (\tau_s + \tau_m) = \tau_m \cdot R_s/(R_s + R_m) = 1.2\ msec$. Moreover, τ_d is in the range $[2.2\ msec, 22\ msec]$. As a consequence, in the critical damping condition τ_{90} was of the order of about 10 msec, a value greater than τ_m itself. As is explained in next paragraph, it follows that the capacitative current $C_m \cdot dV/dt$ recorded during the change of membrane potential was not described by a peak followed by a monoexponential relaxation with time constant τ_m, as happens when $\tau_{90} \ll \tau_m$. Thus the precise value of τ_m and of C_m could not be measured.

6.1.4 V_m dependence on the external K^+ concentration ($[K^+]_o$). A set of experiments on the dependence of the resting membrane potential on the external potassium concentration was performed. The resting potential V_m was continously measured with the voltage recording microelectrode while the bathing solution was changed from Ringer to solutions containing increasing K^+ concentrations (see section 5.4). The osmolarity of the solution was kept constant by simultaneously diminishing the external Na^+ concentration. This latter fact may have an influence on V_m, and will be commented later (see next section).

Two qualitatively different kinds of results were obtained, from a set of 16 oocytes from 4 different donors: the 'K^+ electrode' effect and the 'hyperpolarizing' effect.

The 'potassium electrode' effect consisted in an increasing depolarization of V_m in response to increased $[K^+]_o$. The values of this depolarization varied extensively between oocytes, being very reduced – about 3–5 mV for 70 mM external K^+– in oocytes which had low resting potential ($\sim$ 18–20 mV) in normal Ringer, and more pronounced for oocytes with more negative V_m, e.g. 48 mV decrease for 70 mM external K^+ in an oocyte with -72 mV

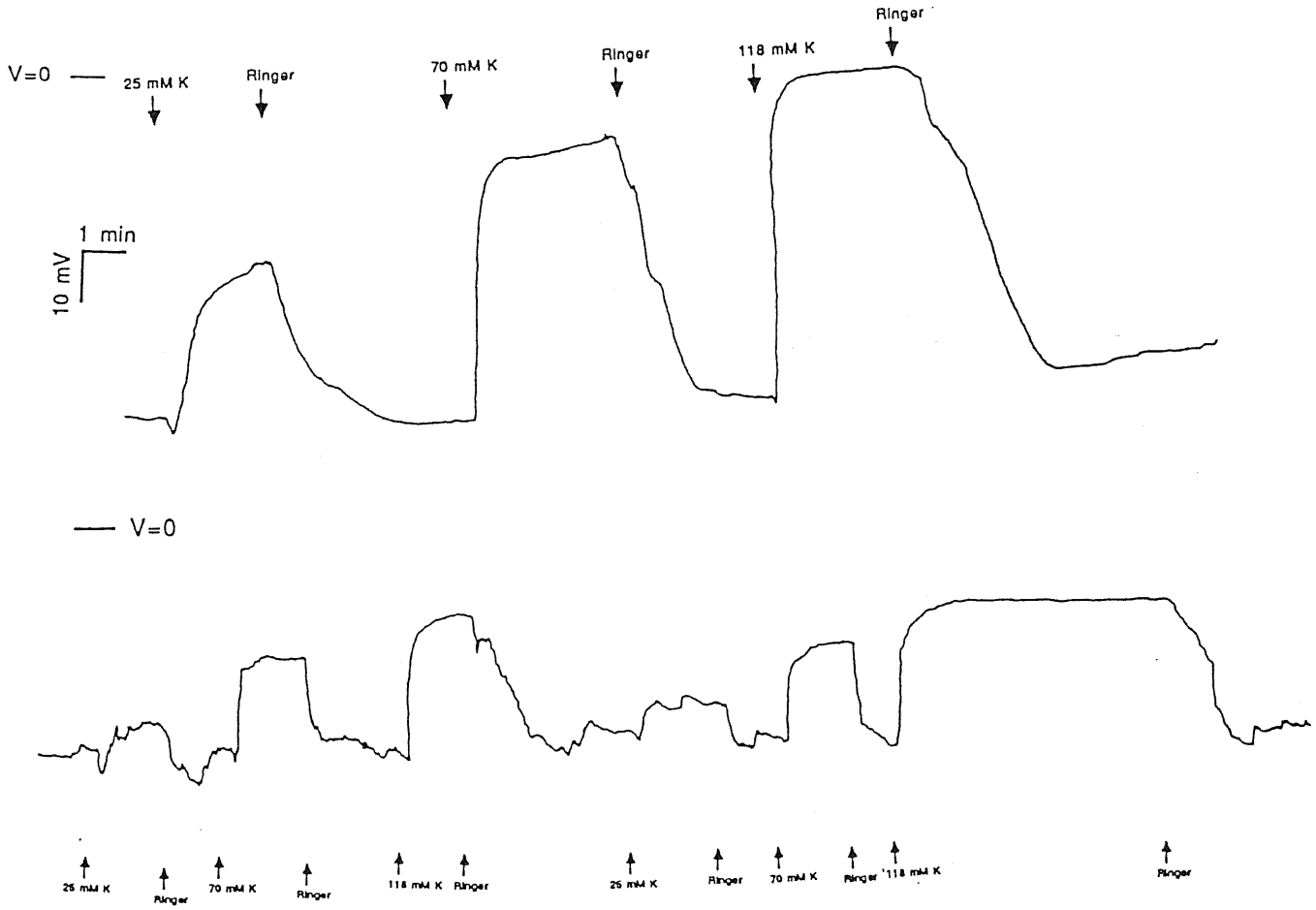

Fig. 6.6: Membrane potential depolarizing responses to $[K^+]_o$ variations. The oocytes were bathed in Ringer and, at the times marked by the arrows, the bath solution was changed either to 25, 70 or 118 mM $[K^+]_o$.

resting potential in Ringer (fig. 6.6).

An explanation of this effect can be given on the basis of the Goldman–Hodgkin–Katz (GHK) equation (see section 2.1). If one assumes that the internal potassium, sodium and chloride concentrations (we approximate the activities with the concentrations) are fixed to the physiological values of 121.5, 18.2 and 62.4 mM for $[K^+]_i, [Na^+]_i$ and $[Cl^-]_i$ respectively (data taken from Kusano et al., 1982), then with normal external concentrations, as those present in a Ringer solution, the Nernst equilibrium potentials for the three ions are $E_k = -98.1$ mV for K^+, $E_{Na} = 46.5$ mV for Na^+, and $E_{Cl} = -16.7$ mV for Cl^-. It follows from the GHK equation that V_m will assume a value in the range [-98.1 mV, 46.5 mV]. Its exact value is determined by the balance between the different permeabilities for potassium

(P_k), sodium (P_{Na}) and chloride (P_{Cl}). If P_k is much greater than the other permeabilities, then $V_m \sim E_k$. In this latter hypothesis, if we raise $[K^+]_o$ so that E_k approaches zero, V_m will be lowered to zero.

In a first approximation we can thus say that in the oocytes showing the 'K^+ electrode' effect the potassium permeability was much higher than the permeability of the other ions, and it determined the V_m decrease. But the V_m decrease with $[K^+]_o$ did not follow exactly the $E_k/[K^+]_o$ Nernst relation, i.e. the behaviour predicted for V_m by the GHK equation when $P_{Na} = P_{Cl} = 0$. The deviation of V_m from E_k gives an idea of the magnitude of the sodium and chloride permeability relative to P_k (P^r_{Na}, P^r_{Cl}).

In 12 over 16 oocytes we could see a depolarization induced by the raise of $[K^+]_o$. In these experiments from the V_m variations we extracted P^r_{Na} and P^r_{Cl}.

To compute the latters, we evaluated $C \equiv V_m - E_k$, and following the GHK equation we equated

$$C = \frac{RT}{F} ln \left[\frac{1 + P^r_{Na} \frac{[Na^+]_o}{[K^+]_o} + P^r_{Cl} \frac{[Cl^-]_i}{[K^+]_o}}{1 + P^r_{Na} \frac{[Na^+]_i}{[K^+]_i} + P^r_{Cl} \frac{[Cl^-]_o}{[K^+]_i}} \right] . \qquad (6.1.5)$$

Rearranging,

$$exp\left\{\frac{CF}{RT}\right\} = \frac{1 + P^r_{Na} \frac{[Na^+]_o}{[K^+]_o} + P^r_{Cl} \frac{[Cl^-]_i}{[K^+]_o}}{1 + P^r_{Na} \frac{[Na^+]_i}{[K^+]_i} + P^r_{Cl} \frac{[Cl^-]_o}{[K^+]_i}} . \qquad (6.1.6)$$

For the estimate of the internal activities of Na^+, Cl^- and K^+ we used data from the literature (Kusano et al., 1982) .

The value of $[Cl^-]_o$ was fixed in all our measures to 121.1 mM, and we controlled the $[Na^+]_o$ and $[K^+]_o$ values so that the relation $[Na^+]_o = (117.5 - [K^+]_o)$ mM held constantly.

In the hypothesis that all the permeabilities were constant during the experiments, and taking in account the above relation between $[K^+]_o$ and $[Na^+]_o$, eq. 6.1.6 becomes a linear relation between exp(CF/RT) and $1/[K^+]_o$. In our measurements we knew $1/[K^+]_o$, we measured C and computed exp(CF/RT), T being $293°K$. We fitted the data with a straight line, whose intercept and a slope, a and b respectively, were related to P^r_{Na} and

P^r_{Cl} by

$$a = \frac{1 - P^r_{Na}}{1 + P^r_{Na}\frac{[Na^+]_i}{[K^+]_i} + P^r_{Cl}\frac{[Cl^-]_o}{[K^+]_i}}$$
$$b = \frac{P^r_{Na} \cdot 117.5 + P^r_{Cl}[Cl^-]_i}{1 + P^r_{Na}\frac{[Na^+]_i}{[K^+]_i} + P^r_{Cl}\frac{[Cl^-]_o}{[K^+]_i}} \qquad (6.1.7)$$

as can be seen after simple algebraic manipulations. Equations 6.1.7 define an algebraic system in the two unknowns P^r_{Na} and P^r_{Cl}. We resolved it in a few cases. For the two measurements reported in fig. 6.6, P^r_{Cl} and P^r_{Na} were 0.14, 0.03 and 0.94, 0.06 respectively.

This great variability could be a sign of the very poor experimental control of some parameters as for example the values of $[Cl^-]_i, [K^+]_i$ and $[Na^+]_i$ and their constancy with time. It is indeed possible that variations of the internal concentrations were produced due to the damage caused to the membrane by mechanical instabilities, or by the leak of KCl from the pipette.

The second kind of V_m behaviour observed in response to $[K^+]_o$ variations was an hyperpolarization of extremely variable amplitude, when $[K^+]_o$ was raised from 2.5 mM (in Ringer) to 20–100 mM (see fig. 6.7). In some oocytes where the hyperpolarization was observed, a subsequent raise of $[K^+]_o$ to 117.5 mM produced the depolarization of V_m expected from a high P_K.

A qualitative explanation is proposed in section 6.2.

In a few cases, the response of V_m to Ach $10^{-5}M$ bath perfusion was tested. In some cases the response was a 18–20 mV depolarization developed in $\sim$ 3–4 minutes; in other cases the response was a 10–12 mV hyperpolarization developed in $\sim$ 1 minute (fig. 6.8). No detailed analysis of the Ach effects was yet undertaken. It is known that the Ach responses are due to muscarinic receptors in the oocyte membrane (Kusano et al., 1977). The muscarinic responses have been extensively studied since the first report of Kusano et al. (1977). For a review, see Miledi, 1988.

6.2 Discussion

The purpose of the work reported in the last section was to test the efficiency of our apparatus for voltage clamping the oocytes, including the

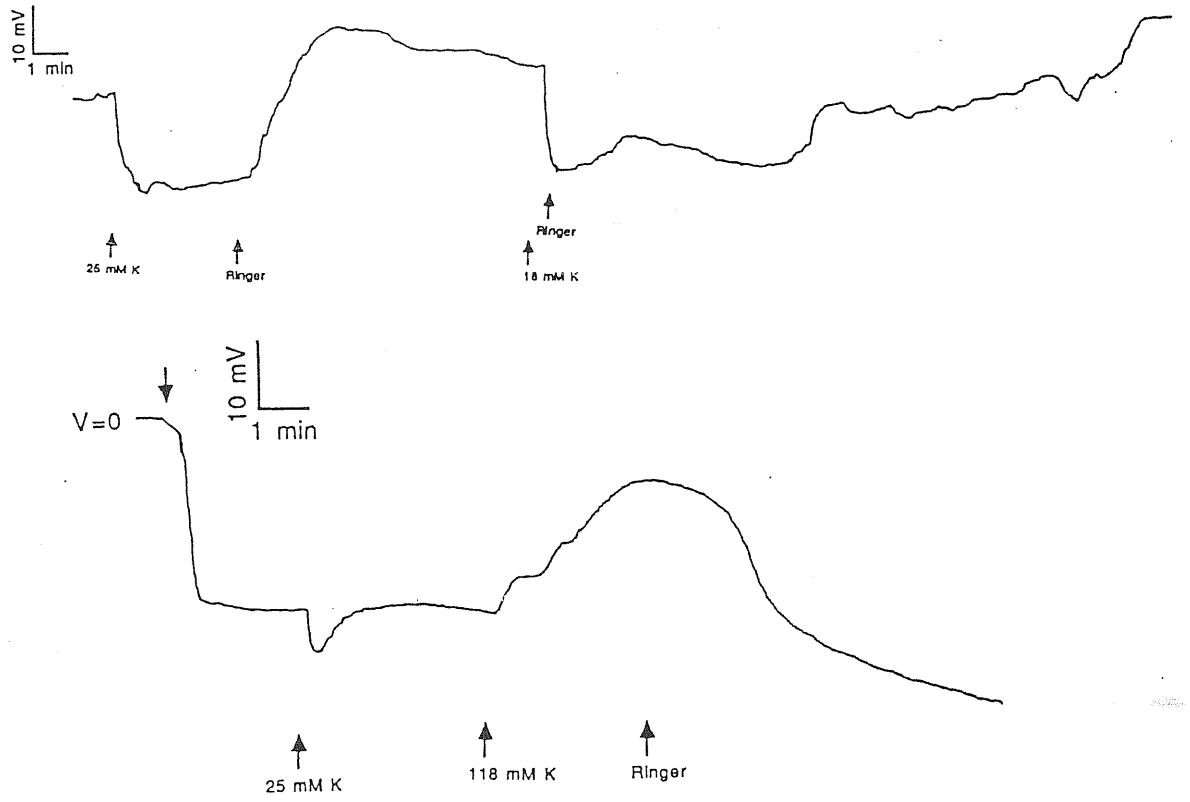

Fig. 6.7: Membrane potential hyperpolarization following bath perfusion with high potassium solutions at times marked by the arrows. Control bath solution is normal Ringer. In B the perfusion with 125 mM $[K^+]_o$ depolarizes the membrane, while 20 mM $[K^+]_o$ has an hyperpolarizing effect.The first arrow from left marks the time of microelectrode insertion in the membrane.

voltage clamp amplifier, the set–up, and the quality of oocytes.

We did not attempt to make an accurate study of the oocyte membrane 'passive' electrical characteristics; moreover such a study was already undertaken in the past by different groups of researchers (Moreau et al., 1976; Belle et al., 1977; Wallace and Steinhardt, 1977; O'Connor et al., 1977; Robinson, 1979; Kado et al., 1981; Lee and Steinhardt, 1981; Baud et al.,

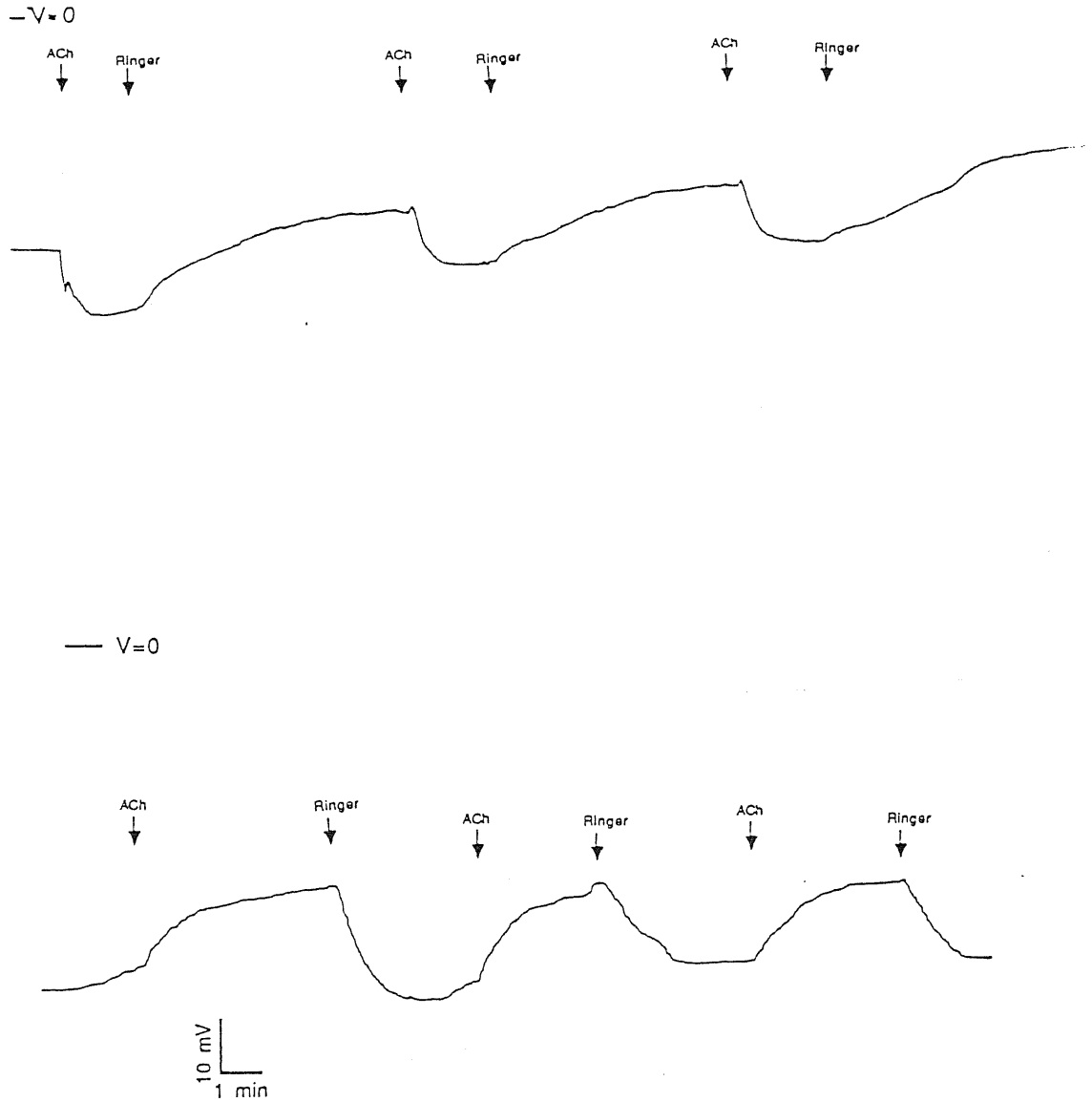

Fig. 6.8: The effect of *Ach* $10^{-5}M$ on the membrane potential. In A, acetylcholine hyperpolarizes V_m. In B the effect is reversed.

1982; Miledi, 1982; Dascal et al., 1984; Costa et al., 1989). We then referred to the data reported by Dascal et al., (1984), Kusano et al., (1982), and Costa et al., (1989), as to model data, to which we compared our results. Our data conerning the characteristics of V_m and of R_m show evident deviations from the results in that literature. These deviations helped us to identify the structural problems of our experimental set–up.

In this discussion thus we expose a critical analysis of the experimental problems affecting our results.

6.2.1 Resting potential. After the insertion of the voltage recording microelectrode in the oocyte membrane typically the recorded voltage showed a

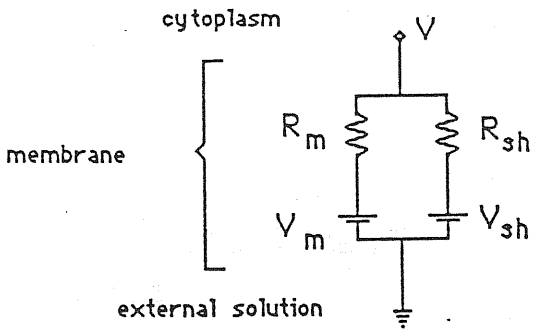

Fig. 6.9: Equivalent circuit illustrating the electrode leakage effect on the resistive membrane current pathways.

slow recovery ($\sim$ 10–20 min). This effect was often reported (see Kusano et al., 1982; Dascal et al., 1984) and is very well studied by Dascal et al. (1984). These authors propose that the effect of the insertion is to open in the membrane a new path for the flow of resistive current. This path can be modeled by a shunt resistance and a battery with e.m.f. V_{sh} in parallel with the normal membrane resistance R_m and e.m.f. V_m (see fig. 6.9). The path would consist of the hole produced by the microelectrode; the slow resealing of the membrane around the pipette would produce the observed repolarization of the measured resting potential V up to the true value V_m. The linear relation $V = R_{input}/R_m \cdot (V_m - V_{sh}) + V_{sh}$ would hold, and this is confirmed in the experimental R_{input}/V relation. The value of V_{sh} is computed by the GHK equation, with the assumption that the new path has no ionic selectivity, so that $P_{Na} = P_{Cl} = P_K$. It follows $V_{sh} = -13.1$ mV, and this fits well the data.

Dascal et al. (1984) also report that the depolarization following a pipette insertion was a very reproducible effect, and it is possible to observe it repetitively in an oocyte by inserting and withdrawing many times a pipette while monitoring the membrane potential with a second microelectrode. These authors did not consider for further measurements the oocytes which did not show a recovery of V_m, as they were thought to be eccessively damaged by the insertion.

Though we did not assess the pipette insertion effect by monitoring it with two micropipettes, we often saw the slow recovery of V_m, and it is very likely that its explanation is the electrode leak artifact just reported.

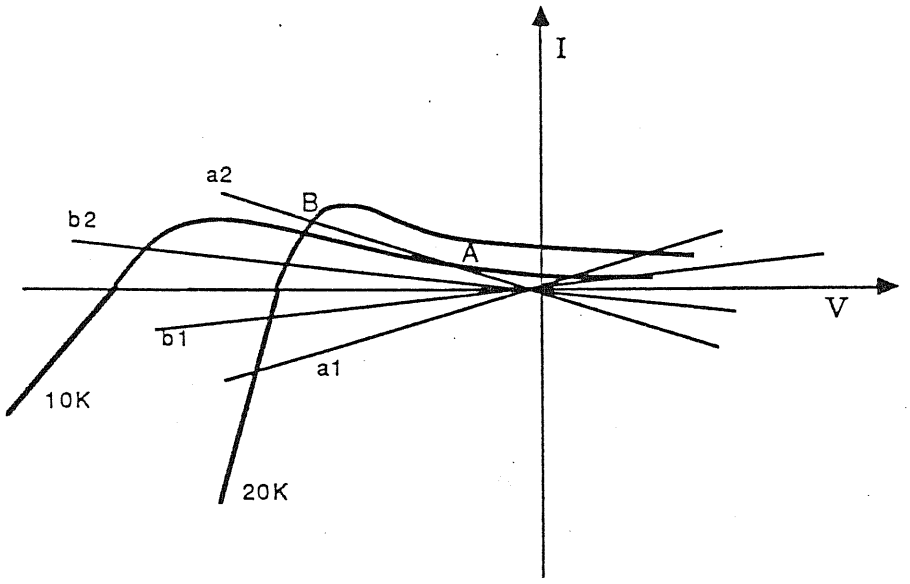

Fig. 6.10: Effect of leakage on the membrane potential dependence on $[K^+]_o$ (see text).

The V_m fluctuations sometimes observed could be partly due to a difficult resealing of the membrane.

$V_m/[K^+]_o$ relations. The V_m hyperpolarization sometimes observed after raising $[K^+]_o$ is an unexpected result. A qualitative explanation of this phenomenon could be found in the combination of three different effects.

The first effect is studied by Hagiwara and Jaffe (1979) and is a consequence of the electrode leak. Suppose that the resting K^+ permeability of a membrane results from a K^+ conductance g_K which has a non linear steady state current–to–voltage characteristic with a negative slope conductance region, as happens for example with the I_{K1} current (Katz, 1949; Hagiwara and Takahashi, 1974).

The I_K–V curve is modified by changes of $[K^+]_o$ by a shift of the V–axis intercept E_k, as is exemplified in fig. 6.10 for 10 mM $[K^+]_o$ (curve 10K) and 20 mM $[K^+]_o$ (curve 20K). Let us make the simplifying assumption that K^+ is the only permeable ion. The resting potential V_m is determined by $I_m = I_K = 0$, where I_m is the total membrane current. Then $V_m = E_k$.

If now a parallel leakage current I_{leak} is added to I_m, then the resting potential will be determined by the condition $I_K + I_{leak} = 0$, or $I_K = -I_{leak}$.

We can graphically search for the intersection of the I_K/V and $-I_{leak}/V$ curves in the I–V plane (see fig. 6.10). If the leakage is represented by the a_1 straight line, then the $-I_{leak}/V$ curve (a_2 in the figure) intersects the two curves 10K and 20K in points A and B respectively. It can be seen that point B corresponds to a more negative voltage value. Thus the effect of raising $[K^+]_o$, together with a sufficiently high leakage conductance, is an hyperpolarization of V_m. If the leakage conductance is instead very low (curves b_1 and b_2), then the V_m value follows approximately the E_k shift with $[K^+]_o$.

This leak artifact could be very strongly contributing to the hyperpolarization seen in our oocytes, as it is very probable that the leak conductance was fairly high. This is in turn suggested by the very low R_m values found.

A second effect contributing to the 'K^+ hyperpolarization' could be the activation of electrogenic pumps. We omitted up to now to consider the pumps currents in the equation determining the membrane resting potential. This latter should correctly be written as

$$I_m = I_{pumps} + I_{leak} + I_{ionic} = 0 \qquad (6.2.1)$$

(the GHK equations corresponds only to $I_{ionic} = 0$). Pumps are present in the oocyte membrane, and the effect of their block has been tested electrophysiologically (Dascal et al., 1984). The pump block with ouabain 10^{-4} M produces depolarization of the membrane, suggesting the block of an outward pump current. Moreover, the $Na^+ - K^+$ pump is partially inhibited at very low $[K^+]_o$ (Wallace and Steinhardt, 1977; Dascal et al., 1984). Therefore the raise of $[K^+]_o$ brings the pump to an increased transport rate and finally to saturation. If $[K^+]_o$ is under the threshold for the pump saturation, then the effect of raising $[K^+]_o$ on I_p is in the direction of a membrane hyperpolarization.

It has been proved with labelled Na^+ flux studies (Tupper and Maloff, 1973; O'Connor et al., 1977) and with electrophysiological ion substitution experiments (Dascal et al., 1984; Costa et al., 1989) that the Na^+ permeability in the oocyte membrane is relatively high with respect to values typical of skeletal muscle and nerve ($P^r_{Na} = 0.01$, see Hodgkin and Katz, 1949; Hodgkin and Horowitz, 1959). In fact, Dascal et al. (1984) report $P^r_{Na} = 0.12$ in follicles and 0.24 in denuded oocytes; Costa et al. (1989) report $P_{Na} = 5.37 \cdot 10^{-8}\ cm \cdot sec^{-1}$, corresponding to $P^r_{Na} = 0.3$, for follicles, and $P_{Na} = 3.75 \cdot 10^{-8}\ cm \cdot sec^{-1}, P^r_{Na} = 0.3$ for denuded oocytes.

In physiological conditions, it turns out that Na^+ importance is comparable to that of K^+ in oocyte resting potential determination. A $[Na^+]_o$ decrease from the physiological value of 115 mM produces hyperpolarization in the membrane potential (see Dascal et al., 1984). It is thus incorrect to use $[Na^+]_o$ as a substitute for $[K^+]_o$ to keep osmolarity constant if one wants to study the K^+ effect on the resting potential. By the way, interestingly it has been proved that not only the sodium permeability is relevant in the oocyte membrane, but also substances as N–methyl–D–glucamine (NMG), choline, sulphate, gluconate and isethionate, traditionally used as impermeant substitutes of potassium, sodium and chloride, are relevantly permeable (Costa et al., 1989). Care should then be taken in designing any ion substitution experiment with oocytes.

In our measurements, the high $[K^+]_o$ solutions were correspondingly sodium depleted. So this is a third possible explanation of the observed hyperpolarization in response to raised $[K^+]_o$. It is true that in the two computations of P^r_{Na}, P^r_{Cl} presented in section 6.1.4, the values obtained for P^r_{Na} are low (0.03 and 0.06). Those results are in conflict with the hypothesis of a high Na^+ permeability; but however they were obtained from oocytes where only the 'K^+ electrode' effect, and no hyperpolarization, was produced by raising $[K^+]_o$. Moreover, the computation of section 6.1.4 is approximate in that it does not take into account the pump effect on V_m. It would be necessary to repeat the measurements after blocking the pumps with ouabain for a more reliable result for P^r_{Na}.

Finally, the input resistance measurements in our voltage clamp experiments gave very low values for R_m, supporting strongly the hypothesis that an excessive damage to the oocytes membrane, and consequently an electrode leak artifact produced a sistematic error in our measurements. This damage could be caused by an incorrect shape of the pipettes, by mechanical vibrations in the set–up, by the intrisic difficulty in the penetration of the oocyte membrane, which resists elastically to the pipette tip insertion (see section 5.5), so that it easily happens to miscalculate the pipette movement.

In our experience the viability of the oocytes was not determined by the number of days passed after extraction from the frog ovary in the range from 0 to 4–5 days after extraction.

Acknowledgements

I would like to thank Prof. Antonio Borsellino for giving me the opportunity to perform this work in the Biophysics Laboratory at S.I.S.S.A. Thanks to Dr.Oscar Moran for many teachings and advices. A thank to Marina Sciancalepore and Zheng Xin for helping me to become acquainted with working in a laboratory, and to Gilberto Giugliarelli and Pasquale Pavone for their friendly support in writing this thesis. Michael Pusch has helped me to understand some faults of my experimental procedure, and I thank him for the patient assistance. I would like to thank Francesca Aicardi for the kindness and help provided me in the two years spent at S.I.S.S.A.; Prof. Fabio Ruzzier of the University of Trieste for kindly supplying me with some experimental materials. Many thanks also to Dr.Bernardini of the University of Milano for supplying me with the frogs and with useful advices on their treatment, and to Dr.Mario Trujillo for help in managing with the construction of electronic instruments.

References

Adrian, R.H., Chandler, W.K. and Hodgkin, A.L. (1970). 'Voltage clamp experiments in striated muscle fibers'. J. Physiol. (Lond.) 208:607–644

Barish, M., (1983).'A transient calcium–dependent chloride current in the immature *Xenopus* oocyte. J.Physiol. (Lond.) 342 : 309–325.

Barnard, E., and Bilbe, G. (1987). 'Functional expression in the *Xenopus* oocyte of mRNAs for receptor and ion channels'. In 'Neurochemistry: a Practical Approach'. A.J. Turner and H. Bachelard eds., IRL Press, Oxford, pp. 243–270.

Baud, C., Kado, R.T. and Marcher, K. (1982). 'Sodium channels induced by depolarization of the *Xenopus laevis* oocyte'. Proc. Nat. Acad. Sci. U.S.A. 79:3188–3192.

Belle, R., Ozon, R. and Stinnakre, J. (1977). 'Free calcium in full grown *Xenopus laevis* oocyte following treatment with ionophore A23187 or progesterone'. Mol. Cell. Endocrinol. 8:65–72.

Bernstein, J. (1902). 'Untersuchungen zur Thermodynamik der bioelektrischen Ströme. Erster Teil'. Pflügers Arch. 82:521–562.

Bertolaccini, M., Bussolati, C. and Manfredi, P.F. (1975). 'Elettronica per misure industriali'. CLUP, Milano

Byerly, L. and Hagiwara, S. (1982). 'Calcium currents in internally perfused nerve cell bodies of *Limnea stagnalis*'. J. Physiol. (Lond.) 322:503–528

Chandler, W.K., Fitzhugh, R. and Cole, K.S. (1962). 'Theoretical stability properties of a space–clamped axon'. Biophys. J. 2:105

Chandler, W.K. and Meves, H. (1965). 'Voltage clamp experiments on internally perfused giant axons'. J. Physiol. (Lond.) 180:788–820

Claudio, T. (1989). 'Molecular genetics of acetylcholine receptor–channels'. In: 'Molecular Neurobiology', D.M. Glover and B.D. Hames eds., IRL Press, Oxford, pp. 63–142.

Cole, K.S. (1949). 'Dynamic electrical characteristics of the squid axon membrane'. Arch. Sci. Physiol. 3:253–268

Cole, K.S. (1972). 'Membrane, ions and impulses'. Univ. of California Press, Berkeley, pp. 569.

Cole, K.S. and Curtis, H.J. (1938). 'Electric impedance of *Nitella* during activity'. J.Gen. Physiol. 22:37–64.

Cole, K.S. and Moore, J.W. (1960). 'Ionic currents measurements in the squid giant axon'. J. Gen. Physiol. 44:123–167

Costa, P.F., Emilio, M.G., Fernandes, P.L., Gil Ferreira, H. and Gil Ferreira, K. (1989). 'Determination of ionic permeability coefficients of the plasma membrane of *Xenopus laevis* oocytes under voltage clamp'. J. Physiol. (Lond.) 413:199–211.

Dascal, N., Landau, E.M. and Lass, Y. (1984). '*Xenopus* oocyte resting potential, muscarinic responses and the role of calcium and guanosine 3'–5'–cyclic monophosphate'. J. Physiol. (Lond.) 352 : 551–574.

Dumont, J.N. (1972). 'Oogenesis in *Xenopus laevis* (Daudin). I. Stages of oocyte development in laboratory maintained animals. J. Morphol. 136: 153–180.

Dumont, J.N. and Brumett, A.R. (1978). 'Oogenesis in *Xenopus laevis* (Daudin). V. Relationship between developing oocytes and their investing follicular tissues'. J. Morphol. 155: 73–98.

Finkel, A.S. and Redman, S.J. (1984). 'Theory and operation of a single microelectrode voltage clamp'. J. Neurosci. Methods 11:101–127

Finkelstein, A. and Mauro, A. (1977). 'Physical principles and formalism of electrical excitability'. In: 'Handbook of Physiology', Sect. 1:'The

Nervous system', vol. 1, Part 1, E.R. Kandel ed., American Physiological Society, Washinghton, D.C..

Ganetzky, B. and Wu, C.–F. (1989). 'Molecular approaches to neurophysiology in *Drosophila*'. In: 'Molecular Neurobiology', D.M. Glover and B.D. Hames eds., IRL Press, Oxford, pp. 9–61.

Gurdon, J.B., Lane, C.D., Woodland, H.R. and Marbaix, G. (1971). 'Use of frog eggs and oocytes for the study of messenger RNA and its translation in living cells'. Nature, 233:177–182.

Halliwell, J.V., Plant, T.D. and Standen, N.B. (1987). 'Voltage clamp techniques'. In: 'Microelectrode techniques'. N.B. Standen, P.T.A. Gray and M.J. Whitaker eds., The Company of Biologists Limited, Cambridge, UK

Hamill, O.P., Marty, A., Neher, E., Sakmann, B. and Sigworth, F.J. (1981). 'Improved patch–clamp techniques for high–resolution current recording from cells and cell–free membrane patches'. Pflügers Arch. 391:85–100

Hille, B. (1983). 'Ionic channels of excitable membranes'. Sinauer Associates Inc., Sunderland, Massachusetts

Hille, B. and Campbell, D.T. (1976). 'An improved vaseline gap voltage clamp for skeletal muscle fibers'. J. Gen. Physiol. 67:265–293

Hagiwara, S. and Jaffe, L.A. (1979). 'Electrical properties of egg cell membranes'. Ann. Rev. Biophys. Bioeng. 8:385–416.

Hagiwara, S. and Takahashi, K. (1974). J. Membr. Biol. 18:61–80.

Hodgkin, A.L. and Horowicz, P. (1959). 'The influence of potassium and chloride ions on the membrane potential of single muscle fibers'. J. Physiol. (Lond.) 148:127–160.

Hodgkin, A.L. and Katz, B. (1949). 'The effect of sodium on the electrical activity of the giant axon of the squid'. J. Physiol. (Lond.) 108:37–77.

Kado, R.T., Marcher, K. and Ozon. R. (1981). 'Electrical membrane properties of the *Xenopus laevis* oocyte during progesterone–induced meiotic maturation'. Develop. Biol. 84:471–476.

Katz, B. (1949). Arch. Sci. Physiol. 3:283–300.

Kusano, K., Miledi, R. and Stinnakre, J. (1977). 'Acetylcholine receptors in the oocyte membrane'. Nature, 270:739–741.

Kusano, K., Miledi, R. and Stinnakre, J. (1982). 'Cholinergic and catecholaminergic receptors in the *Xenopus* oocyte membrane'. J. Physiol. (Lond.) 328:143–170.

Lee, S.C. and Steinhardt, R.A. (1981). 'pH changes associated with meiotic maturation in oocytes of *Xenopus laevis*'. Develop. Biol. 85:358–369.

Hodgkin, A.L. and Huxley, A.F. (1952). 'A quantitative description of membrane current and its application to conduction and excitation in nerve'. J. Physiol. (Lond.) 117:500–544.

Hodgkin, A.L., Huxley, A.F. and Katz, B. (1952). 'Measurements of current–voltage relation in the membrane of the giant axon of *Loligo*'. J. Physiol. (Lond.) 116:424–448

Kado, R.T., Marcher, K. and Ozon. R. (1981). 'Electrical membrane properties of the *Xenopus laevis* oocyte during progesterone–induced meiotic maturation'. Develop. Biol. 84:471–476.

Katz, G.M. and Schwartz, T.L. (1974). 'Temporal control of voltage–clamped membranes: an examination of principles'. J. Membrane Biol. 17:275–291

Korn, A.G. and Korn, T.M. (1968). 'Mathematical Handbook for Scientists and Engeneers'. McGraw–Hill Book Company

Kostyuk, P.G. and Krishtal, O.A. (1984). 'Intracellular perfusion of excitable cells'. In: 'Methods in the Neurosciences', IBRO handbook series, vol. 5, Chichester, Wiley

Kusano, K., Miledi, R. and Stinnakre, J. (1982). 'Cholinergic and catecholaminergic receptors in the *Xenopus* oocyte membrane'. J. Physiol. (Lond.) 328:143–170.

Linear Databook 1 (1988). National Semiconductor Corporation, Santa Clara, California.

Lubbert, H., Hoffman, B.J., Snutch, T.P. VanDyke, T., Levine, A.J., Hartig, P.R., Lester, M.A. and Davidson, N. (1987). 'cDNA cloning of a serotonin 5–HT_{lc} receptor by electrophysiological assays of mRNA injected *Xenopus* oocytes. Proc. Natl. Acad. Sci. U.S.A. 84:4332–4336.

Marmont, M. (1949). 'Studies on the axon membrane'. J. Cell. Comp. Physiol. 34:351–382

Maru, Y., Nakayama, K., Tamaki, M., Marada, Y., Kuno, M. and Nakanishi, S. (1987). 'cDNA cloning of bovine substance–K receptor through oocyte expression system'. Nature 329:836–838.

Methfessel, C., Witzemann, T., Takahashi, T., Mishina, M., Numa, S. and Sakmann, B. (1986). 'Patch clamp measurements on *Xenopus* laevis oocytes: currents through endogenous channels and implanted acetylcholine receptor and sodium channels'. Pflügers Arch. 407:577–588.

Miledi, R. (1982). 'A calcium–dependent transient outward current in *Xenopus laevis* oocytes'. Proc. Roy. Soc. (London) B 215:491–497.

Miledi, R., Parker, I. and Sumikawa, K. (1983). 'Recording of single γ–aminobutyrate– and acetylcholine–activated receptor channels translated by exogenous mRNA in *Xenopus* oocytes'. Proc. Roy. Soc. (London) B 218:481–484.

Miledi, R., Parker, I. and Sumikawa, K. (1989). 'Transplanting receptors from brain into oocytes'. In: 'Fidia Award Lecture Series'. J. Smith ed., Raven Press, New York

Mishina, M., Kurosaki, T., Tobimatsu, T., Morimoto, Y., Noda, M., Yamamoto, T., Terao, M., Lindstrom, J., Takahashi, T., Kuno, M. and

Numa, S. (1984). 'Expression of functional acetylcholine receptor from cloned cDNAs'. Nature 307:604–608.

Mishina, M., Tobimatsu, T., Tanaka, K., Fujita, Y., Fukuda, K., Kurasake, M., Takahashi, H., Morimoto, Y., Hirose, T., Inayama, S., Takahashi, T., Kuno, M. and Numa, S. (1985). 'Location of functional regions of acetylcholine receptor α–subunit by site–directed mutagenesis'. Nature 313:364–369.

Moore, J.W. (1971). 'Voltage clamp methods'. In: 'Biophysics and Physiology of Excitable Membranes'. W.J. Adelman Jr. editor. Van Nostrand Reinhold Co., New York.

Moore, J.W. and Cole, K.S. (1963). 'Voltage clamp techniques'. In: 'Physical Techniques in Biological Research', W.L. Nastuck editor, Academic Press Inc., New York.

Moreau, M., Guerrier, P. and Doree, M. (1976). 'Modifications precoces des proprietes electriques de la membrane plasmique des ovocytes de *Xenopus laevis* au cours de la reinitiations meiotique induite par la progesterone, la parachlormercuribenzoate (pCMB) ou l'ionophore A23187'. Comp. Rend. Acad. Sci., Paris D282:1209–1312.

Nonner, W. (1969). 'A new voltage clamp method for Ranvier nodes'. Pflügers Arch. 309:176–192

O'Connor, C.M., Robinson, K.R. and Smith, L.D. (1977). 'Calcium, potassium and sodium exchange by full–grown and maturating *Xenopus laevis* oocytes'. Develop. Biol. 61:28–40.

Purves, R.D. (1981). 'Microelectrode Methods for Intracellular Récording and Ionophoresis'. Academic Press, London, pp. 146; ch.3–5.

Robinson, K.R. (1979). 'Electrical currents Through full–grown and maturating *Xenopus* oocytes'. Proc. Nat. Acad. Sci. U.S.A. 76:837–841.

Smith, T.G., Barker, J.L., Smith, B.M. and Colburn, T.R. (1980). 'Voltage clamping with microelectrodes'. J. Neurosci. Methods 3:105–128

Sumikawa, K., Houghton, M., Emtage, J.S., Richards, B.M. and Barnard, E.A. (1981). 'Active multi–subunit Ach receptor assembled by translation heterologous mRNA'. Nature, 292:862–864.

Sumikawa, K., Parker, I. and Miledi, R. (1986). '*Xenopus* oocytes as a tool for molecular cloning of the genes coding for neurotransmitter receptors and voltage–operated channels'. In:'Membrane control of cellular activity', H.Ch. Luttgau ed., Prog. in Zool. 33:127–139.

Sumikawa, K., Parker, I. and Miledi, R. (1989). 'Expression of Neurotransmitter Receptors and Voltage–Activated Channels from Brain mRNA in *Xenopus* oocytes'. In: 'Methods in Neuroscience', Vol I. Academic Press Inc.

Sumikawa, K., Parker, I. and Miledi, R. (1988). 'Effect of tunicamycin on the expression of functional brain neurotransmitter receptors and voltage–operated channels in *Xenopus* oocytes'. Molec. Brain Res. 4:191–199.

Sumikawa, K. and Miledi, R. (1989). 'Assembly and N–glycosylation of all Ach receptor subunits are required for their efficient insertion into plasma membranes'. Molec. Brain Res. 5:183–192.

Taglietti, V. and Toselli, M. (1988). 'A study of stretch–activated channels in the membrane of frog oocytes: interactions with Ca^{++} ions'. J. Physiol. (Lond.) 407 : 311–328.

Taylor, R.E., Moore, J.W. and Cole, K.S. (1960). 'Analysis of certain errors in squid axon voltage clamp measurements'. Biophys. J. 1:161

Timpe, L.C., Schwarz, T.L., Tempel, B.L., Papazian, D.M., Jan, Y.N. and Jan, L.Y. (1988). 'Expression of functional potassium channels from *Shaker* cDNA in *Xenopus* oocytes'. Nature 331:143–145.

Tupper, J.T. and Maloff, B.L. (1973). 'The ionic permeability of the amphibian oocyte in the presence or absence of external calcium'. J. Exp. Zool. 184:321–334.

Wallace, R.A. and Steinhardt, R.A. (1977). 'Maturation of *Xenopus*

oocytes. II. Observations on membrane potential'. Develop. Biol. 57:305–316.